THE JOURNAL OF BIOLOGICAL CHEMISTRY VOL. 289, NO. 49, pp. 34308–34324, December 5, 2014

Presynaptic Control of Glycine Transporter 2 (GlyT2) by Physical and Functional Association with Plasma Membrane Ca^{2+}-ATPase (PMCA) and Na^{+}-Ca^{2+} Exchanger (NCX)*

Received for publication, June 5, 2014, and in revised form, September 29, 2014 Published, JBC Papers in Press, October 14, 2014, DOI 10.1074/jbc.M114.586966

Jaime de Juan-Sanz[‡], Enrique Núñez[§¶‖], Francisco Zafra[§¶‖], María Berrocal[**], Isaac Corbacho[**], Ignacio Ibáñez[§¶‖], Esther Arribas-González[§¶‖], Daniel Marcos[**], Beatriz López-Corcuera[§¶‖], Ana M. Mata[**], and Carmen Aragón[§¶‖1]

From the [‡]Department of Biochemistry, Weill Cornell Medical College, New York, New York 10065, the [§]Centro de Biología Molecular "Severo Ochoa," Universidad Autónoma de Madrid, Consejo Superior de Investigaciones Científicas, 28049-Madrid, Spain, the [¶]Centro de Investigación Biomédica en Red de Enfermedades Raras, ISCIII, 46009-Valencia, Spain, the [‖]IdiPAZ-Hospital, Universitario La Paz, 28046-Madrid, Spain, and the [**]Departamento de Bioquímica y Biología Molecular y Genética, Facultad de Ciencias, Universidad de Extremadura, 06006-Badajoz, Spain

Background: GlyT2 is crucial for glycinergic neurotransmission, but only a few interacting partners for this protein are known.
Results: PMCA2/3 and NCX1 interact with GlyT2 and modulate its activity in lipid raft subdomains.
Conclusion: Functional interaction of GlyT2 with PMCA2/3 and NCX1 helps Na^{+} and Ca^{2+} local homeostasis in glycinergic terminals.
Significance: Learning how GlyT2 is regulated might help with developing new therapies for hyperekplexia or neuropathic pain.

Fast inhibitory glycinergic transmission occurs in spinal cord, brainstem, and retina to modulate the processing of motor and sensory information. After synaptic vesicle fusion, glycine is recovered back to the presynaptic terminal by the neuronal glycine transporter 2 (GlyT2) to maintain quantal glycine content in synaptic vesicles. The loss of presynaptic GlyT2 drastically impairs the refilling of glycinergic synaptic vesicles and severely disrupts neurotransmission. Indeed, mutations in the gene encoding GlyT2 are the main presynaptic cause of hyperekplexia in humans. Here, we show a novel endogenous regulatory mechanism that can modulate GlyT2 activity based on a compartmentalized interaction between GlyT2, neuronal plasma membrane Ca^{2+}-ATPase (PMCA) isoforms 2 and 3, and Na^{+}/Ca^{2+}-exchanger 1 (NCX1). This GlyT2·PMCA2,3·NCX1 complex is found in lipid raft subdomains where GlyT2 has been previously found to be fully active. We show that endogenous PMCA and NCX activities are necessary for GlyT2 activity and that this modulation depends on lipid raft integrity. Besides, we propose a model in which GlyT2·PMCA2–3·NCX complex would help Na^{+}/K^{+}-ATPase in controlling local Na^{+} increases derived from GlyT2 activity after neurotransmitter release.

Glycine is a major inhibitory neurotransmitter of the CNS that acts in neuronal circuits of the central auditory pathway, receptive fields in the retina, and spinal cord-sensitive pathways. Glycinergic synaptic inhibition is terminated by two sodium- and chloride-coupled transporters, GlyT1[2] and GlyT2, located in the glial plasma membrane and presynaptic terminals, respectively (1, 2). Additionally, GlyT2 transport activity supplies glycine for presynaptic vesicle refilling, a process that is absolutely necessary to preserve quantal glycine content in synaptic vesicles (3–5). GlyT2 activity dysfunctions reduce presynaptic glycine release and cause significant lacking of inhibitory glycinergic neurotransmission. In humans, this situation causes hyperekplexia or startle disease, a rare disease that is characterized by an exaggerated startle response, usually evoked by tactile or auditory stimuli, leading to hypertonia and apnea episodes that in some cases produce sudden infant death (6–8). GlyT2 has a crucial role in the pathophysiology of inhibitory glycinergic neurotransmission, and studying modulatory factors that regulate its activity might help the success of future therapies. Indeed, studies of endogenous GlyT2 regulatory mechanisms have revealed that GlyT2 activity is regulated by PKC activation (9, 10), lipid raft environment (10, 11), P2Y purinergic receptors (12), ubiquitination (13), calnexin function (14), or Na^{+}/K^{+}-ATPase interaction (15). In addition, we have also described that GlyT2 exocytosis is regulated by syntaxin-1A and calcium (Ca^{2+}) increases (16). Ca^{2+} ions are widely known essential regulators of synaptic function because of the following: (*a*) synaptic neurotransmitter release is driven by Ca^{2+} influxes through voltage-gated calcium channels (17, 18), and (*b*) Ca^{2+} ions have an important role as secondary

* This work was supported by Spanish Dirección General de Investigación Científica y Técnica Grants SAF2008-05436 and SAF2011-28674, Fondo de Investigaciones Sanitarias (Centro de Investigación Biomédica en Red de Enfermedades Raras) and Fundación Ramón Areces (to C. A. and B. L. C.), and Ministerio de Economía y Competitividad, Junta de Extremadura, and Fondo Europeo de Desarrollo Regional Grants BFU2011-23313 from (to A. M. M.).

[1] To whom correspondence should be addressed: Centro de Biología Molecular "Severo Ochoa," Universidad Autónoma de Madrid, 28049-Madrid, Spain. Tel.: 34-91-1964632; Fax: 34-91-1964420; E-mail: caragon@cbm.csic.es.

[2] The abbreviations used are: GlyT1, glycine transporter 1; GlyT2, glycine transporter 2; PMCA, plasma membrane Ca^{2+}-ATPase; NCX, Na^{+}-Ca^{2+} exchanger; NKA, Na^{+}/K^{+}-ATPase; SERCA, sarco(endo)plasmic reticulum; SPCA, secretory pathway; DRM, detergent-resistant membrane; ANOVA, analysis of variance; BAPTA, 1,2-bis(2-aminophenoxy)ethane-*N*,*N*,*N*′,*N*′-tetraacetic acid tetrakis(acetoxymethyl ester); KB-mes, KB-R7943 mesylate; MβCD, methyl-β-cyclodextrin.

messengers in numerous signal transduction processes (19–21). Thus, neurons invest large amounts of energy in controlling and maintaining an abrupt gradient between intracellular (~0.1-μM) and extracellular (~1.4-mM) Ca^{2+} concentrations. Plasma membrane calcium ATPases (PMCAs) have the key biochemical function of extruding cytosolic Ca^{2+} out of the cell (by the spent of ATP) in a calmodulin-stimulated manner (22–24). These Ca^{2+} pumps belong to the P-type ATPase superfamily that also encompasses, for example, the Na^+/K^+-ATPase (NKA) or the Ca^{2+}-ATPases of the sarco(endo)plasmic reticulum (SERCA) (25) and the secretory pathway (SPCA) (26). Four different genes have been described (*ATP2B1–4*) that encode four PMCA isoforms (PMCA1–4), and the average amino acid sequence identity amounts to only about 80% (27, 28). The four PMCA isoforms show differential patterns of expression, with PMCAs 1 and 4 being ubiquitously expressed and PMCAs 2 and 3 being expressed predominantly in the CNS (29, 30). The distribution of PMCA isoforms in isolated DRMs (or lipid rafts) is a point of controversy because in synaptic plasma membranes (SPMs) from pig cerebellum PMCA4 seems to be the only isoform located in raft domains (31), although in primary cortical neurons (32) or hippocampus membranes[3] all isoforms appear to be raft-associated. Recently, Jiang *et al.* (33) have described by quantitative mass spectrometry that the four isoforms are associated with rafts in synaptic plasma membranes from whole rat brain, representing about 60% of the total PMCA. This DRM-associated PMCA pool has been shown to have higher specific activity (32–35) according to the initial proposition that PMCAs are more active when included in these membrane subdomains (36). Similarly, we have described that GlyT2 can be found in DRMs where it displays the highest transport activity (11) suggesting that GlyT2 presence/absence in lipid rafts could be a versatile regulatory mechanism for the transporter (9, 10).

In this study, we have identified neuronal PMCA isoforms 2 and 3 and the Na^+/Ca^{2+} exchanger (NCX1) as new interacting and regulatory partners of GlyT2. We found that GlyT2, PMCA2/3, and NCX1 are co-enriched in neuronal lipid raft membrane clusters. Pharmacological inhibition of PMCA activity by the specific inhibitor caloxin 2a1, as well as specific inhibition of the reverse mode of NCX by KB-R7943 mesylate (KB-mes), led to a marked reduction in GlyT2 activity suggesting that proper Ca^{2+} extrusion in presynaptic terminals is somehow necessary for optimal GlyT2 activity. This PMCA/NCX regulation of GlyT2 depends on lipid raft integrity because lipid raft disruption by methyl-β-cyclodextrin (MβCD) blocks caloxin 2a1 and KB-mes effects and reduces co-localization of NCX and PMCAs with GlyT2. Here, we suggest that the local functional coupling between GlyT2, PMCA2/3, and NCX1 occurs in lipid raft domains and that this association may help in correcting the local imbalance of Na^+ produced during high activity periods of 1glycine-3Na^+ co-transport by GlyT2 after neurotransmitter release. These local increases in cytosolic Na^+ could not be entirely covered by the Na^+/K^+-ATPase activity due to its slow Na^+-extruding rate (200 s^{-1}) (37) forcing NCX to extrude Na^+ at its normal higher speed (5000 s^{-1}) (38, 39) and producing local Ca^{2+} increases that will be amended by PMCA activity.

EXPERIMENTAL PROCEDURES

Materials

Male Wistar rats were bred under standard conditions at the Centro de Biología Molecular Severo Ochoa in accordance with the current guidelines for the use of animals in research. All animal procedures were approved by the institutional animal care committee and performed according to European Union guidelines (Council Directive 2010/63/EU). Antibodies against GlyT2 were obtained in-house (rabbit and rat (1, 40)), although the other primary antibodies used were as follows: anti-PMCA2, anti-PMCA3, anti-PMCA4, and anti-PMCA (clone 5F10) from Thermo Scientific; anti-Thy-1 (Pharmingen); anti-flotillin1 (BD Biosciences); anti-clathrin heavy chain (BD Transduction Laboratories); PSD95 (Neuromab); and anti-NCX1 (Swant). Fluorophore-coupled secondary antibodies were from Molecular Probes. All chemicals used were from Sigma unless otherwise noted, and Neurobasal medium and B-27 supplement were purchased from Invitrogen. Caloxin 2a1 (VSNSNWPSFPSSGGG-NH_2) (41) was custom-synthesized by the proteomics service of the Centro de Biología Molecular Severo Ochoa (Madrid, Spain).

Immunoprecipitation

Synaptosomes or primary neurons from the brainstem or spinal cord (100 μg) were lysed for 30 min at room temperature at a concentration of 1.5 mg of protein/ml in TN buffer (25 mM Tris-HCl and 150 mM NaCl (pH 7.4)) containing 0.25% Nonidet P-40 and protease inhibitors (0.4 mM phenylmethylsulfonyl fluoride (PMSF) + Sigma mixture). After 15 min of centrifugation in a microcentrifuge to remove the cell debris, 4 μg of protein were separated to quantify total protein, and 5 μl of the primary antibody were added and left overnight at 4 °C using the following antibodies for immunoprecipitation: rat anti-GlyT2, anti-PMCA (clone 5F10), or anti-NCX1. A negative control was also run in parallel in which an irrelevant antibody was added, denoted as IgG. Subsequently, 50 μl of 50% protein G-agarose beads (ABT Beads) were added and incubated for 45 min at 4 °C. The beads were collected by mild centrifugation and washed twice for 7 min with lysis buffer at room temperature. Finally, the beads were pelleted, and the immunoprecipitated proteins were eluted in Laemmli buffer at 75 °C for 10 min, resolved in SDS-polyacrylamide gels (7.5%), detected in Western blots by ECL, and quantified on a GS-810 imaging densitometer (Bio-Rad). The amount loaded was always 4 μg of total protein and 96 μg of immunoprecipitated sample or IgG immunoprecipitation controls. This ratio allows having both samples in the same linear range of exposure.

Primary Cultures of Brainstem and Spinal Cord Neurons

Primary cultures of brainstem and spinal cord neurons were prepared as described previously (13, 15).

[3] D. Marcos and A. M. Mata, unpublished data.

Immunofluorescence of Primary Neurons and Synaptosomes from Rat Brainstem and Spinal Cord

Primary neurons or purified synaptosomes were analyzed by immunofluorescence as reported previously (15). The primary antibodies used in this work were incubated overnight at 4 °C using the following dilutions: GlyT2 (1:500); PSD95 (1:500); PMCA2 (1:250); PMCA3 (1:150); NCX1 (1:200); and Thy-1 (1:500). The cells were visualized by confocal microscopy on an inverted microscope Axiovert200 (Zeiss).

Immunohistochemistry of Rat Brainstem Slices

Immunohistochemistry experiments from rat brainstem slices were performed as described previously (42). The sections shown in this work correspond to the ventral cochlear nucleus of the brainstem.

[^{3}H]Glycine Transport Assays in Brainstem and Spinal Cord Synaptosomes

Uptake assays in brainstem and spinal cord synaptosomes were performed in constant mild shaking at 37 °C in PBS containing 2 μCi/ml [^{3}H]glycine (1.6 TBq/mmol; PerkinElmer Life Sciences), cold glycine (1 μM final concentration), plus 10 μM *N*[3-(4′-fluorophenyl)-3-(4′-phenylphenoxy)propyl]sarcosine to inhibit glycine transport by GlyT1 (IC_{50} = 16 nM) with or without the specific GlyT2 inhibitor ALX1393 (0.5 μM, IC_{50} = 50 nM) to measure background glycine accumulation. After incubating 20 μg of synaptosomes for 7 min with radioactive medium, synaptosomes were recovered using 0.45-μm nitrocellulose filters (Millipore), washed three times, and prepared for scintillation counting. All assays were performed at least in triplicate and expressed as mean ± S.E.

Ca^{2+}-ATPase Activity Measurement in Brainstem and Spinal Cord Synaptosomes

The Ca^{2+}-ATPase activity was measured using a coupled assay in different conditions to measure the contribution of PMCA and the intracellular SERCA and SPCA ATPases as described in Sepúlveda *et al.* (43).

Immunofluorescence Quantification, Generation of Color Maps, and Generation of Pixel Fluorescence Intensity Profiles

At least 45 images for each condition were quantified using ImageJ software (National Institutes of Health). Images were processed with a 2.0-pixel median filter, and the threshold used was automatically determined by the JACoP plugin (44). The Pearson's value was obtained with JACoP by comparing the two thresholded channels and measuring the correlation between them. The value can range from −1 to 1, with 1 representing the maximal co-localization possible (two identical images), whereas values ≥0.5 can usually be considered as valid co-localization (45). Co-localization color maps were generated in ImageJ using the co-localization color map plugin (46). Pixel fluorescence intensity profiles were also generated using ImageJ software. The linear region of interest was manually drawn to cross several GlyT2-PMCA/NCX-Thy-1 clusters, and the fluorescence intensity profiles were obtained from each individual color channel using the RGB_profiler plugin. Intensity profile plots were generated in Origin 8.0 (Figs. 5 and 8, *green*, PMCAs/NCX1; *red*, GlyT2; *blue*, Thy-1), and triple co-localization spots were considered valid only when intensity values of the three proteins were higher than 65% of the maximum at the same region.

Mass Spectrometry Assays

In-Gel Digestion—In-gel digestion was performed as described previously (47, 48).

Reverse Phase-Liquid Chromatography RP-LC-MS/MS Analysis (Dynamic Exclusion Mode)—The desalted protein digest was dried, resuspended in 10 μl of 0.1% formic acid, and analyzed by RP-LC-MS/MS in an Easy-nLC II system coupled to an ion trap LTQ-Orbitrap-Velos-Pro mass spectrometer (Thermo Scientific). The peptides were concentrated by reverse phase chromatography using a 0.1 × 20-mm C18 RP precolumn (Proxeon) and then separated using a 0.075 × 100-mm C18 RP column (Proxeon) operating at 0.3 μl/min. Peptides were eluted using a 90-min gradient from 5 to 40% solvent B (solvent A: 0.1% formic acid in water, and solvent B: 0.1% formic acid, 80% acetonitrile in water). ESI ionization was done using a Nano-bore emitter stainless steel inner diameter of 30 μm (Proxeon) interface. The Orbitrap resolution was set at 30,000.

Peptides were detected in survey scans from 400 to 1600 atomic mass units (1 microscan), followed by 15 data-dependent MS/MS scans (top 15), using an isolation width of 2 units (in mass-to-charge ratio units), normalized collision energy of 35%, and dynamic exclusion applied during 30-s periods. Peptide identification from raw data was carried out using the SEQUEST algorithm (Proteome Discoverer 1.3, Thermo Scientific). Database search was performed against uniprot-rattus.fasta. The following constraints were used for the searches: tryptic cleavage after Arg and Lys, up to two missed cleavage sites, and tolerances of 10 ppm for precursor ions and 0.8 Da for MS/MS fragment ions, and the searches were performed allowing optional Met oxidation and Cys carbamidomethylation. Search against decoy database (integrated decoy approach) was performed using a false discovery rate of <0.01.

Lipid Raft Isolation

Membrane rafts were biochemically isolated from brainstem and spinal cord synaptosomes as described previously (10). Quantification of the relative distribution in lipid rafts of the different proteins was performed as shown in Equation 1,

$$\text{raft} = \frac{R}{R+NR}\cdot 100;\ \text{non-raft} = \frac{NR}{R+NR}\cdot 100 \qquad \text{(Eq. 1)}$$

where R is the raft optical density/μg of protein, and NR is the non-raft optical density/μg of protein. Densitometric analyses were performed on at least three independent Western blots representing the means ± S.E.

Data Analysis

All statistical analyses were performed using Origin 8.0 (OriginLab Corp.). One-way analysis of variance (ANOVA) was

A

Short name	Accession	Description	# AAs	MW [kDa]	Score	IPGlyT2	IgG
GlyT2	P58295-2	Sodium- and chloride-dependent glycine transporter 2 [SC6A5_RAT]	791	86,99	60,10	20	0
PMCA1	P11505-1	Plasma membrane calcium-transporting ATPase 1 [AT2B1_RAT]	1,258	138,72	0,00	0	0
PMCA2	P11506-5	Plasma membrane calcium-transporting ATPase 2 [AT2B2_RAT]	1154	127,28	19,64	7	0
PMCA3	Q64568-12	Plasma membrane calcium-transporting ATPase 3 [AT2B3_RAT]	1115	122,79	18,93	6	0
PMCA4	Q64542-1	Plasma membrane calcium-transporting ATPase 4 [AT2B4_RAT]	1203	133,09	0,00	0	0
SERCA	Q71UZ2	Sarco/endoplasmic reticulum Ca2+-ATPase [Q71UZ2_RAT]	869	95,19	8,89	3	0
Calmodulin	P62161	Calmodulin [CALM_RAT]	149	16,83	6,93	2	0
CamKIIα	P11275	Calcium/calmodulin-dependent protein kinase type II subunit alpha [KCC2A_RAT]	478	54,08	4,70	2	0
CADPS1	F1LLX6	Calcium-dependent secretion activator 1 [F1LLX6_RAT]	1148	129,60	7,32	2	0
SCaM2	Q8K3P6	Calcium-binding mitochondrial carrier protein SCaMC-2 [SCMC2_RAT]	469	52,66	4,80	2	0
UqCrC2	P32551	Cytochrome b-c1 complex subunit 2, mitochondrial [QCR2_RAT]	452	48,37	57,94	13	13

B PMCA3; Unique peptide: IQEAYGDVSGLCR. XCorr:3.21

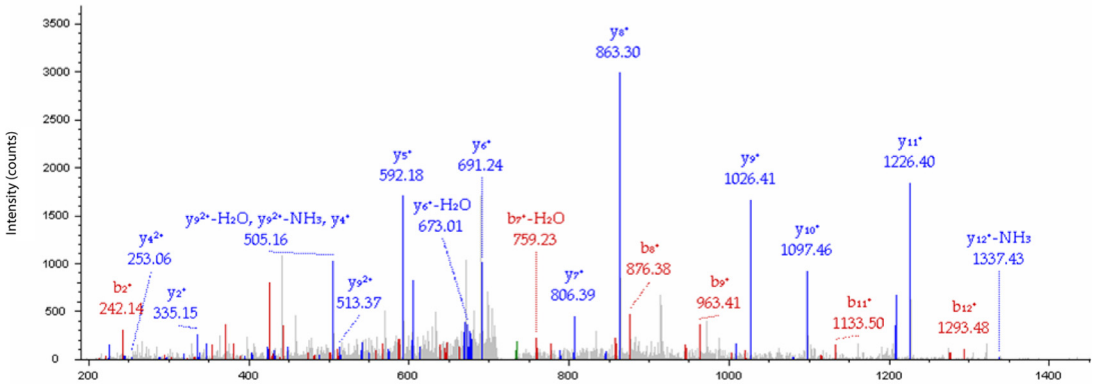

C PMCA2; Unique peptide: TSPVEGLPGTAPDLEK. XCorr:2.92

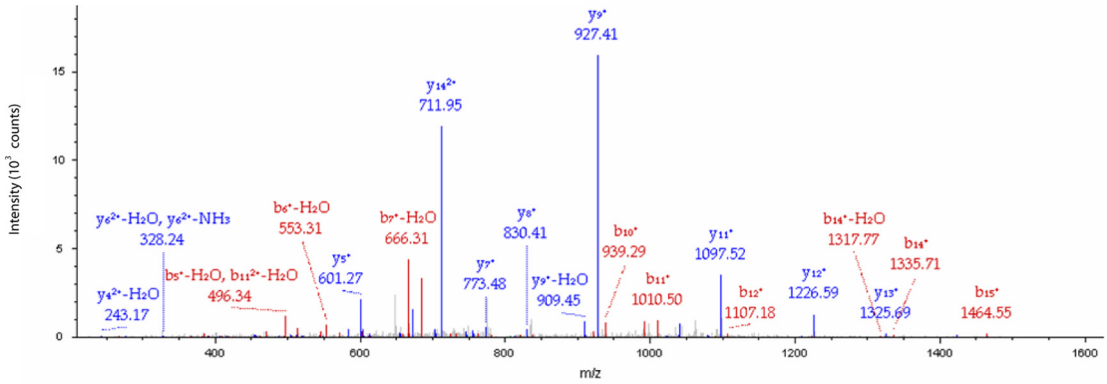

FIGURE 1. **Proteomic identification of PMCA2 and PMCA3 as putative interacting partners of GlyT2.** *A, table* represents the number of peptides obtained from mass spectrometry from GlyT2 immunoprecipitates (IPGlyT2) or control IgG immunoprecipitates (IgG). GlyT2 is shown as an auto-immunoprecipitated positive control, and cytochrome *b*-c_1 complex is shown as an example of a nonspecific interaction that was identified equally in controls and GlyT2 immunoprecipitations. Note the significant number of PMCA2 and PMCA3 peptides identified in GlyT2 immunoprecipitations. *B* and *C,* MS/MS spectra from the double charged ions at *m/z* 734.35, corresponding to the IQEAYGDVSGLCR peptide of PMCA3 (*B*), and 805.92, corresponding to TSPVEGLPGTAPDLEK peptide of PMCA2 (*C*).

used to compare multiple groups, with subsequent Tukey's post hoc test to determine the significant differences between samples. The Student's *t* test was used to compare two separate groups. *p* values are denoted through the text as follows: *, $p < 0.05$; **, $p < 0.01$; ***, $p < 0.001$; and $p < 0.05$ or lower values were considered significantly different when compared by one-way ANOVA (Tukey's post hoc test) or Student's *t* test. When shown, box whisker plots represent the following: median (line); mean (point); 25th to 75th percentile (box); 10th to 90th percentile (whisker); 1st to 99th percentile (×); and minimum to maximum (−) ranges.

RESULTS

Given the pathophysiological important role of GlyT2 (6) and considering the small number of proteins currently known to interact with this transporter, we carried out a proteomic study to identify new molecular partners involved in the functional regulation of GlyT2. Thus, the native transporter was immunoprecipitated from brainstem and spinal cord synaptosomes using a specific GlyT2 antibody (40), and co-purified proteins were identified by high throughput mass spectrometry. GlyT2 immunoprecipitates were found to selectively enhance the detection of several proteins, including some of the

previously described GlyT2 interacting partners such as syntaxin-1 (16) or Na^+/K^+-ATPase (15). We also found other molecules that are known to be implicated in GlyT2 trafficking, such as clathrin heavy chain (10).

Surprisingly, mass spectrometry also revealed other proteins, the main function of which is related to intracellular calcium homeostasis. In this last group, the highest number of specific peptides detected corresponded to the neuron-specific PMCA isoforms 2 and 3 (Fig. 1*A*, highlighted in *red*), which are responsible for extruding calcium out of cells at the expense of ATP and thus regulating cytosolic calcium concentration at nerve terminals (representative tandem mass spectra of PMCA2- and PMCA3-specific peptides obtained in these assays are shown in Fig. 1, *B* and *C*). PMCA2 and PMCA3 have been shown to be richly expressed in synapses (49–52), where they are proposed to control neurotransmission dynamics (via controlling Ca^{2+}-mediated synaptic vesicle fusion) and/or regulate local Ca^{2+} signaling (53, 54).

GlyT2 Interacts with PMCA2 and PMCA3 in Brainstem and Spinal Cord Synaptosomes and in Heterologous Systems—To confirm the interaction between GlyT2 and PMCA2 and 3, we performed reverse immunoprecipitations from brainstem and spinal cord synaptosomal lysates using an antibody that recognizes the four PMCA isoforms (PMCA1–4, clone 5F10) (Fig. 2*A*). Western blotting showed that the antibody selectively immunoprecipitated the respective target protein and that GlyT2 specifically co-purified in PMCA immunoprecipitates (Fig. 2*A*), indicating that native GlyT2 and PMCA proteins interact specifically under physiological conditions. However, proteomic data only pointed out the neuron-specific PMCA isoforms 2 and 3 as putative interacting partners of GlyT2 (Fig. 1), and consequently, we performed further GlyT2 immunoprecipitations and detected PMCA2 and PMCA3 using isoform-specific antibodies (Fig. 2, *B–D*). Western blotting showed a specific co-purification of PMCA2 and PMCA3, yet no signal was observed when an irrelevant antibody was added (denoted as IgG). Furthermore, PMCA4 is not found co-purifying in these conditions (Fig. 2*D*), in agreement with proteomic data.

The interaction between GlyT2 and PMCA2 or PMCA3 was also detected in a heterologous COS7 cell line overexpressing each isoform together with the wild type transporter or with a GlyT2 mutant lacking the C-terminal region, which contains a PDZ (95/Disc large/Zonula occludens-1) ligand motif that could potentially interact with the PDZ binding domain of the pumps, as reported for some PMCA-interacting partners (55–57). Western blot assays (Fig. 2, *E* and *F*) showed that both PMCA2 and PMCA3 clearly maintained their association with the transporter despite the lack of its PDZ-containing C-terminal region, indicating that the PMCA2- and PMCA3-GlyT2 interactions are not PDZ domain-based interactions and suggesting that other regions of GlyT2 are implicated in the physical coupling between both proteins.

To further confirm the interaction between GlyT2 and PMCA2 or PMCA3 in the native system, their co-localization was examined by immunohistochemistry in rat brainstem slices. As shown in Fig. 3, double labeling for GlyT2 and PMCA2 or PMCA3 indicates that GlyT2 clearly co-localizes

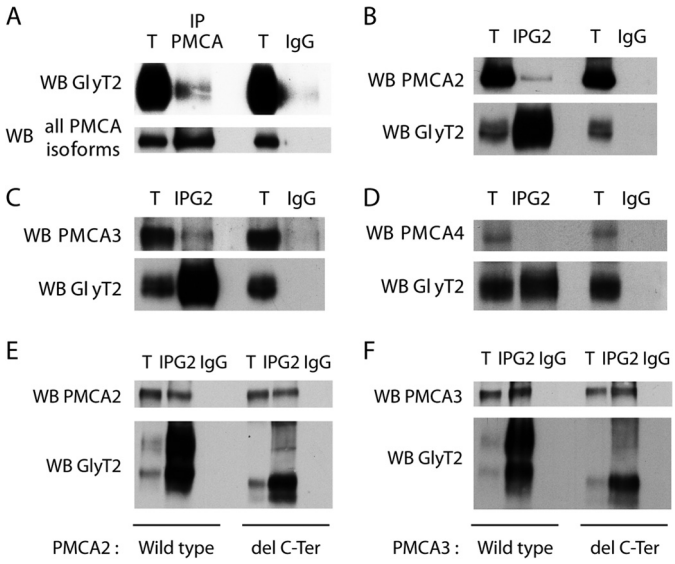

FIGURE 2. **GlyT2 interacts with PMCA2 and PMCA3 in CNS preparations and heterologous cells.** *A–D,* synaptosomes from rat brainstem and spinal cord were lysed and incubated with antibodies against GlyT2 (*B–D*), PMCA (against all isoforms, clone 5F10) (*A*), or the equivalent IgGs as control (*A–D*). Precipitated protein complexes were analyzed by Western blots (*WB*) probed with anti-GlyT2, anti-PMCA (all isoforms), anti-PMCA2, anti-PMCA3, or anti-PMCA4 antibodies. *T,* total protein; *IP,* immunoprecipitated sample; *IgG,* IgG immunoprecipitation controls. Note that an interaction can be detected between GlyT2 and PMCA isoforms 2 and 3, yet no signal is observed in PMCA4 Western blots or in the IgG controls. *E* and *F,* COS7 cells were transfected to express wild type GlyT2 or GlyT2 lacking the C-terminal region (amino acids from 737–799; denoted as *del C-Ter*) and PMCA isoforms 2 or 3. Lysed cells were incubated with antibodies against GlyT2 or the equivalent IgGs as control and protein complexes were precipitated using protein-agarose beads and analyzed in Western blots probed with anti-GlyT2 (*E* and *F*) and anti-PMCA2 (*E*) or anti-PMCA3 (*F*) antibodies. Two bands of wild type GlyT2 are detected when expressed in COS cells as reported previously (14). *T,* total protein; *IP,* immunoprecipitated sample; *IgG,* IgG immunoprecipitation controls. Note that the interaction can still be detected between GlyT2 lacking the C-terminal region and the PMCA isoforms, indicating that the PDZ domain of GlyT2 is not necessary for this interaction.

with PMCA2 (Fig. 3*A*) and PMCA3 (Fig. 3*B*), especially in presynaptic structures (Fig. 3, *A* and *B, detail*). In addition, we performed immunocytochemistry in synaptosomes from brainstem and spinal cord (Fig. 4). Double labeling for GlyT2 and PMCA2 or PMCA3 (Fig. 4, *B* and *C*) indicates that most GlyT2 overlaps with both isoforms, whereas no co-localization is observed with a postsynaptic marker, PSD-95 (Fig. 4*A*). These differences can be quantified using the Pearson's value of correlation, obtaining a significant co-localization between PMCAs and GlyT2 (Fig. 4*D*, PMCA2 Pearson's value: 0.635 ± 0.013 S.E., $p = 1.98 \times 10^{-23}$; PMCA3 Pearson's value: 0.596 ± 0.009 S.E.; $p = 7.97 \times 10^{-22}$). Together, these immunoprecipitation, immunohistochemical, and immunocytochemical results indicate a specific interaction between GlyT2 and the neuronal PMCA2 and PMCA3 isoforms.

GlyT2 and PMCA Isoforms 2 and 3 Are Co-enriched in Neuronal Lipid Raft Membrane Clusters—DRMs or lipid rafts are small (10–200 nm), heterogeneous, highly dynamic, and sterol- and sphingolipid-enriched domains that compartmentalize cellular processes (58–60). GlyT2 displays optimal transport activity when it is associated with these subdomains at the cell surface, where most of the transporter resides in primary neurons and synaptosomes from the rat brainstem (11, 15). Considering that PMCA isoforms are also localized in lipid rafts,

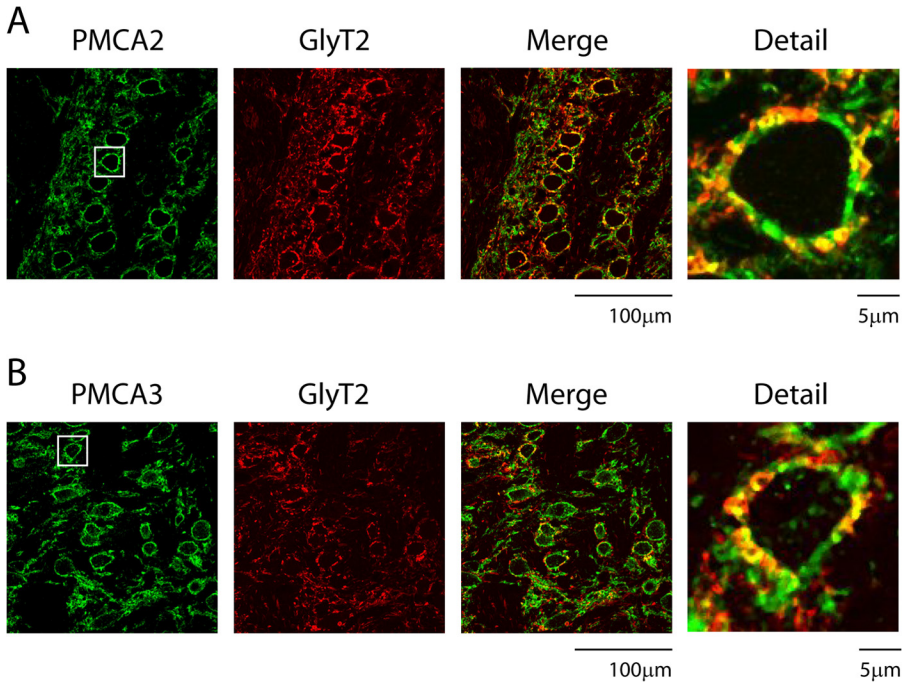

FIGURE 3. **GlyT2 co-localizes with PMCA2 and PMCA3 in brainstem slices.** *A* and *B,* adult rat brainstem slices were fixed and incubated with antibodies against GlyT2 and PMCA2 (*A*) or PMCA3 (*B*). After incubation with the secondary antibodies, the slices were visualized by confocal microscopy, showing GlyT2 in *red* and PMCAs in *green*. Note the co-localization of both proteins, especially in presynaptic structures (ventral cochlear nucleus slices are shown). *Scale bar,* 100 μm. *Scale bar* of detailed images, 5 μm.

where they are known to be optimally active (32–35), we investigated whether the coupling shown here between PMCAs and GlyT2 could be facilitated by membrane subdomain compartmentalization of these proteins. As a first approach, we sought to determine the distribution of GlyT2, PMCA2, and PMCA3 in raft subdomains using sucrose gradient centrifugation. As shown in Fig. 5, the three proteins are distributed among raft and non-raft fractions (Fig. 5, *A* and *B*). In agreement with previously reported results, GlyT2 is enriched in raft fractions (9, 15), showing here a relative distribution in rafts of 77.26 ± 4.46% S.E., whereas PMCA2 and PMCA3 distributions are 51.09 ± 6.25% and 49.46 ± 7.57% S.E., respectively (Fig. 5*B*). Correct biochemical isolation of raft fractions was confirmed by Western blotting of raft and non-raft markers, flotillin1 and clathrin heavy chain, respectively.

To find out whether GlyT2 and PMCA2 or PMCA3 are present in the same raft clusters, we performed immunocytochemical assays in primary neurons using specific antibodies against GlyT2, PMCA2 or PMCA3, and Thy-1, a marker of neuronal rafts (Fig. 5, *C–H*) (61). We observed a clear co-localization between GlyT2 and Thy-1, as reported previously (15). Interestingly, these GlyT2-Thy-1 clusters extensively co-localized with PMCA2 or PMCA3, leading to a high degree of triple co-localization as shown by the white color in the overlay image (denoted as *Merge* in Fig. 5, *D* and *G*). To clearly visualize triple co-localization, we generated color maps that highlight pixels of co-localization (Fig. 5, *D* and *G*) (46) and pixel fluorescence intensity profiles of each individual color staining that show a substantial overlap among the plots of each color staining (Fig. 5, *E* and *H*) (62). In this case, triple co-localization spots are highlighted by inverted arrows. Taken together, these biochemical and immunocytochemical results suggest that GlyT2 and PMCA pumps are associated in lipid raft subdomains, where both proteins have been shown to be optimally active (11, 32–35).

PMCA Function Regulates Presynaptic Glycine Transport by GlyT2—Given that GlyT2 and PMCAs are co-enriched in raft membrane subdomains, where they have been proposed to be fully functional, we next analyzed the possible regulatory interplay between these proteins. As a first approach, we measured GlyT2 and PMCA activities in brainstem and spinal cord synaptosomes in the presence of ALX1393, a specific GlyT2 inhibitor (63). As expected, ALX1393 reduced about 90% of the transporter activity (Fig. 6*A*) but did not affect PMCA activity (Fig. 6*B*), suggesting that PMCA function is independent of GlyT2 activity. We also tested the reverse hypothesis measuring GlyT2 transport in the presence of the PMCA inhibitor caloxin 2a1, which specifically impairs PMCA function in a dose-dependent manner (Fig. 6, *C* and *D*) while not affecting other Ca^{2+}-ATPases such as SERCA or SPCA (Fig. 6*C*) (64, 65). Fig. 7*A* shows that incubation with 400 μM caloxin 2a1 for 10 min produced a significant down-regulation of GlyT2 transport, with the remaining activity of 66.38 ± 2.26% S.E. compared with the control ($p = 1.36 \times 10^{-7}$, *green box plot*). However, the same protocol did not produce any differences when we measured the activity of the highly related glycine transporter GlyT1 (Fig. 7*B*; $p = 0.152$) (1). This suggests a specific regulation of GlyT2 by PMCA activity, indicating that somehow Ca^{2+} extrusion by PMCAs is necessary for optimal GlyT2 glycine recapture. PMCA function is tightly related to the function of the plasma membrane sodium/calcium exchanger (NCX) (66). In virtually all cells, NCX mainly operates in its "forward" mode harnessing the electrochemical gradient of Na^+ to extrude Ca^{2+} with a known stoichiometry of $3Na^+$:

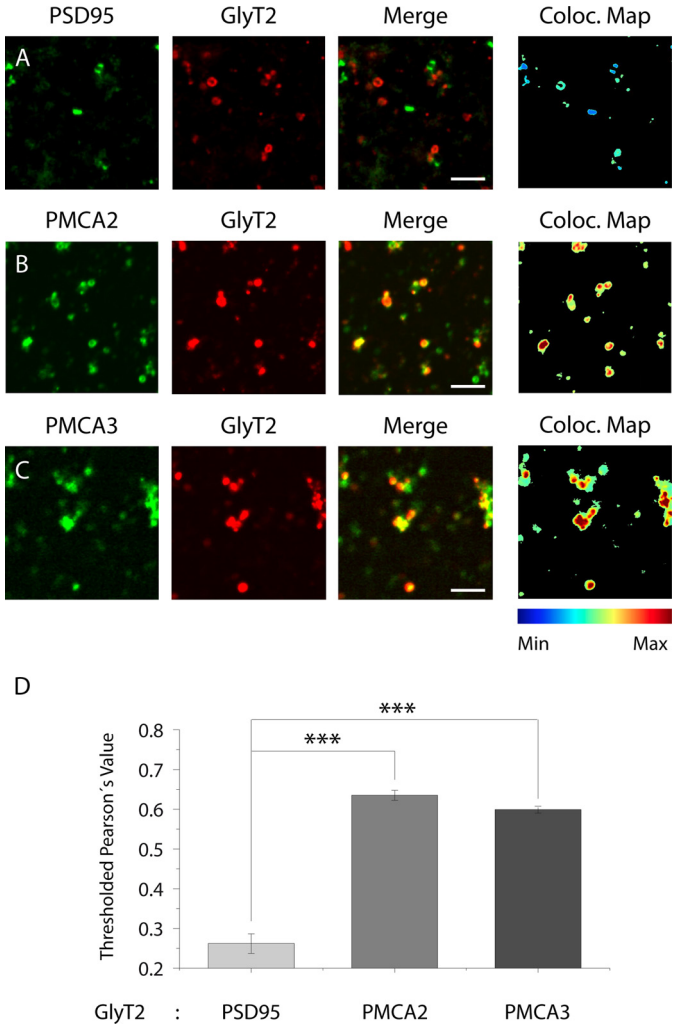

FIGURE 4. **GlyT2 co-localizes with PMCA2 and PMCA3 in synaptosomes from adult rat brainstem and spinal cord.** *A–D,* synaptosomes isolated from the adult rat brainstem and spinal cord were deposited on glass coverslips, fixed, and incubated with antibodies against GlyT2 and PSD95, PMCA2, or PMCA3. Synaptosomes were visualized by confocal microscopy, showing GlyT2 in *red* and PSD95/PMCAs in *green*. *D,* quantification of the co-localization using Pearson's value was performed as described under "Experimental Procedures." The histogram represents the mean ± S.E. ($n = 3$; on average, 30 images per condition were analyzed in each experiment): ***, significantly different, $p < 0.001$ by ANOVA with Tukey's post hoc test. PSD95 is shown as a negative control of no co-localization. *Scale bar,* 3 μm.

$1Ca^{2+}$ (67), helping PMCA proteins in the cytosolic calcium clearance (68, 69). However, during high frequency action potentials in presynaptic terminals, the activity-mediated increase in cytosolic Na^+ can switch NCX direction of flux exchange extruding Na^+ and allowing Ca^{2+} entry (70–72). In this mode, NCX produces local increases in Ca^{2+} concentration that are thought to be corrected by PMCA activity. Based on these data, we hypothesized that PMCA-mediated modulation of GlyT2 transport could be based on NCX locally acting in the reverse mode to correct Na^+ entry mediated by GlyT2 transport, which is known to introduce $3Na^+$ ions per glycine recaptured (73). NCX reverse mode can be pharmacologically inhibited by the isothiourea derivative KB-mes (74–77). Brainstem and spinal cord synaptosomes incubated with KB-mes showed a significant down-regulation of GlyT2 transport (42.99 ± 5.71% S.E.; $p = 1.53 \times 10^{-9}$) in a similar level to that observed in the presence of caloxin 2a1 (66.38 ± 2.26% S.E.; $p = 1.36 \times 10^{-7}$) (Fig. 7*A*, *purple box plot*), indicating that NCX function is also needed for optimal GlyT2 activity and suggesting a PMCA/NCX cooperative effect in regulating GlyT2 transport. Moreover, simultaneous treatment with caloxin 2a1 and KB-mes produced a reduction in GlyT2 activity (49.88 ± 6.17% S.E.) that is not significantly different from KB-mes ($p = 0.9627$) or caloxin 2a1 ($p = 0.17$) treatments alone, further supporting the hypothesis that both proteins are acting in the same pathway (Fig. 7*A*, *light blue box plot*). In addition, to confirm that Ca^{2+} extrusion by PMCAs is necessary for optimal GlyT2 glycine recapture, we used BAPTA-AM, a cell-permeant ion chelator that is a highly selective for Ca^{2+}. Incubation of synaptosomes with BAPTA-AM reduces the availability of cytosolic Ca^{2+} affecting PMCA activity and interfering on the NCX functional shift toward the reverse mode (71). In these conditions, GlyT2 activity appears to be significantly reduced (71.80 ± 6.10% S.E.; $p = 0.00043$), suggesting that cytosolic concentration of Ca^{2+} could affect glycine recapture by affecting NCX/PMCA proteins.

GlyT2 Interacts with NCX1, and Both Proteins Are Present in the Same Neuronal Membrane Raft Clusters—Results from Fig. 7 indicate that NCX functions contribute to GlyT2-mediated glycine recapture in the presynaptic terminal. A working hypothesis of this work is that NCX could act by correcting the local imbalance of Na^+ produced during high activity periods of glycine-Na^+ co-transport by GlyT2 after neurotransmitter release that could not be covered by Na^+/K^+-ATPase due to its slow rate (200^{-1} s) (37). This localized process should be facilitated by the proximity of both proteins, and therefore we sought to determine whether GlyT2 and NCX physically interact and/or are compartmentalized in the same membrane clusters. NCX was not detected in the initial proteomic studies (Fig. 1), not even increasing the false discovery rate to 5% (data not shown). However, some proteins are particularly difficult to detect by mass spectrometry or they can be present in amounts below the detection limit of this technique. Therefore, not finding unique peptides of a protein in immunoprecipitation experiments does not exclude the possibility of a real interaction. To test this putative interaction between GlyT2 and NCX, we performed reverse immunoprecipitations from brainstem and spinal cord synaptosomal lysates using antibodies that recognize NCX1 or GlyT2 (Fig. 8, *A* and *B*). Western blot assays showed that each antibody selectively immunoprecipitated the respective target protein, that GlyT2 was specifically co-purified in NCX1 immunoprecipitates (Fig. 8*A*), and that NCX1 was specifically co-purified in GlyT2 immunoprecipitates (Fig. 8*B*), indicating indeed a physical interaction.

In addition, to find out whether GlyT2 and NCX1 are present in the same raft clusters, immunocytochemical assays were performed in primary neurons using specific antibodies against GlyT2, NCX1, and Thy-1 as done in Fig. 5 for PMCAs (Fig. 8, *C* and *D*). In this case, GlyT2-Thy-1 clusters also extensively co-localized with NCX1, visualized by triple co-localization color maps or pixel fluorescence intensity profiles from each individual protein. Taken together, results from Fig. 8 indicate that NCX1 is physically interacting with

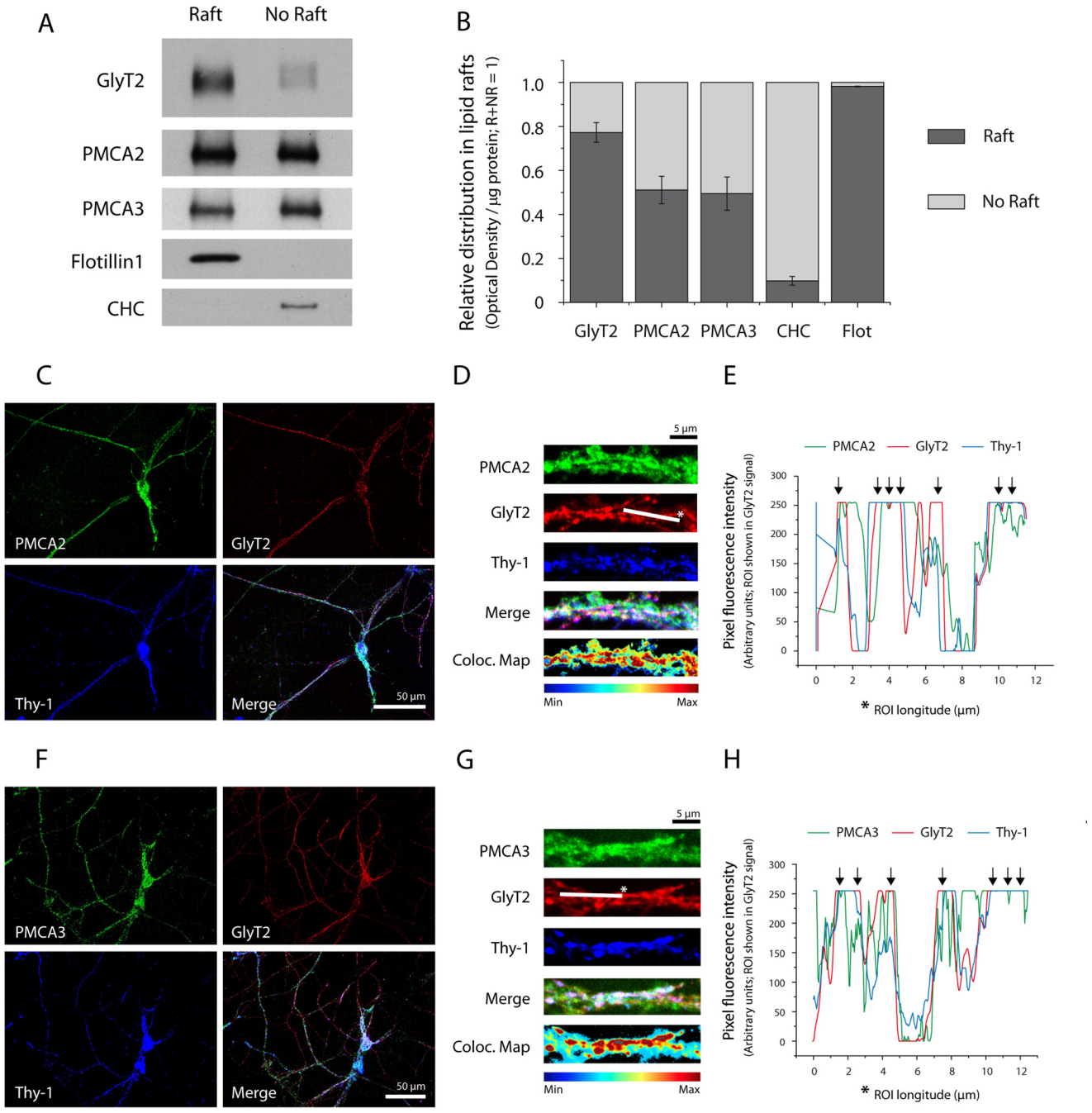

FIGURE 5. **GlyT2 is present in neuronal lipid rafts containing PMCA2 or PMCA3.** *A* and *B*, lipid raft fractions (denoted as *Raft*) were isolated from brainstem and spinal cord synaptosomal lysates and analyzed by Western blot to determine GlyT2, PMCA2, and PMCA3 distribution in lipid rafts. The purity of the isolation was determined probing anti-flotillin1 (raft marker) and anti-clathrin heavy chain (*CHC*, non-raft marker). *B*, histogram shows the quantification of the relative distribution of each protein representing the means ± S.E. from three different experiments as shown in *A*. *C–H*, primary cultures of spinal cord and brainstem neurons were fixed and incubated with primary and secondary antibodies against PMCA2 or PMCA3 (*green*), GlyT2 (*red*), and the lipid raft marker Thy-1 (*blue*). Cells were visualized by confocal microscopy, and amplified high definition images of axonal regions were taken to generate triple co-localization maps (*Coloc. Map*) (*D* and *G*). *E* and *H*, pixel fluorescence intensity profiles were generated to visualize co-distribution of GlyT2 and PMCA2/3 in Thy-1-positive clusters. The linear region of interest was manually drawn from left to right, and fluorescence intensity profiles were obtained from each individual color channel. Triple co-localization spots are highlighted by *inverted arrows*. *Scale bar* in *C* and *F*, 50 µm. *Scale bar* in *D* and *G*, 5 µm.

GlyT2 and suggest that both proteins are present in the same membrane clusters. Therefore, we suggest that GlyT2 is coupled to NCX1 and PMCAs in lipid raft subdomains where both proteins coordinately act in regulating glycine recapture by correcting local Na^+ and Ca^{2+} variations after neurotransmitter release.

PMCA/NCX1 Regulation of GlyT2 Activity Depends on Lipid Raft Integrity—PMCA pumps are optimally active when they are present in lipid raft subdomains (32–35). In addition, GlyT2 is more active when it is raft-associated (11). In this work, we show that PMCA, NCX, and GlyT2 are together in the same raft clusters; therefore, we next sought to assess whether the

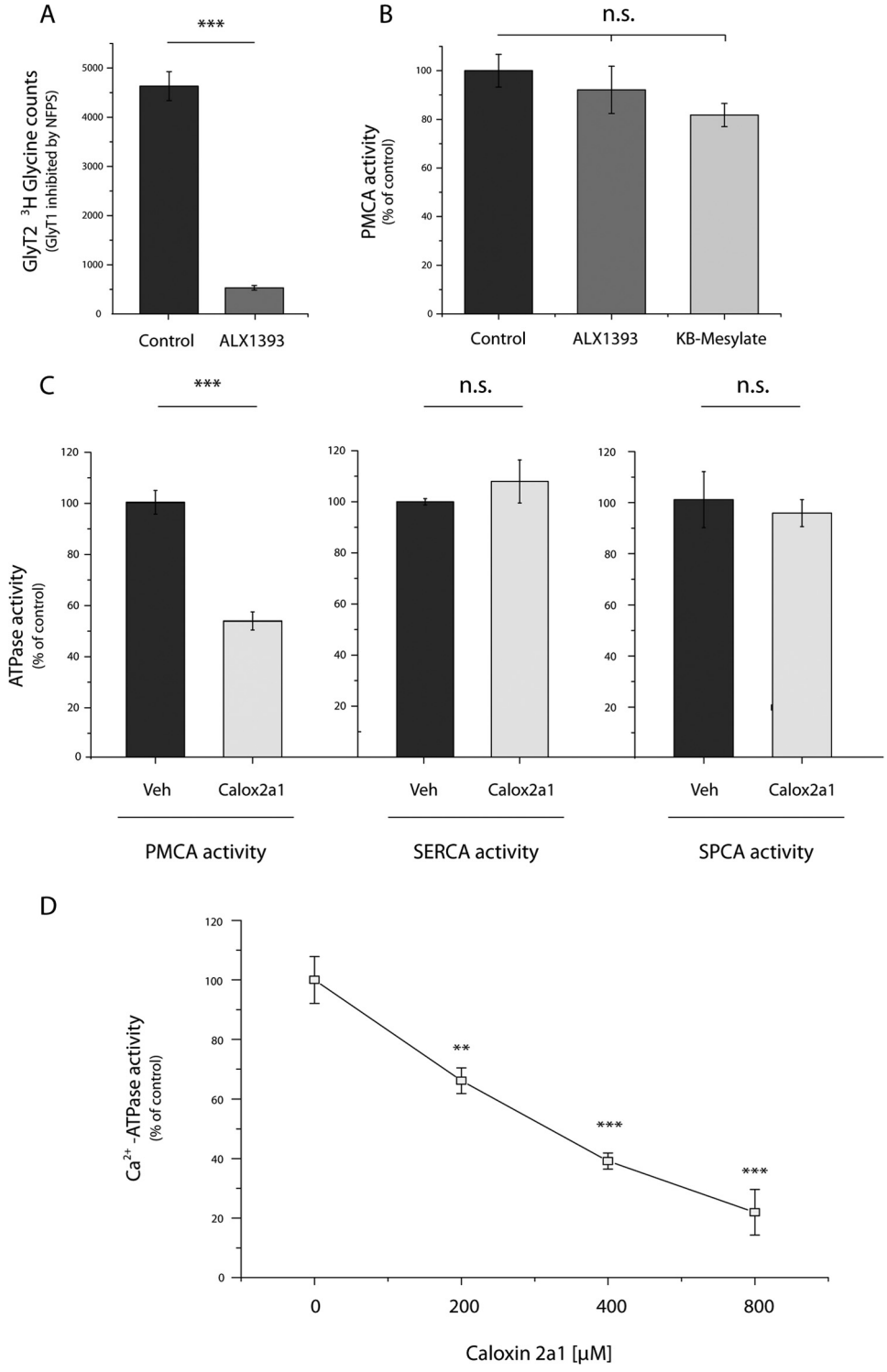

FIGURE 6. **Effects of ALX1393 in PMCA and GlyT2 activities and effects of caloxin 2a1 in Ca^{2+}-ATPase activities in brainstem and spinal cord synaptosomes.** *A–D,* synaptosomes from the rat brainstem and spinal cord were isolated and incubated with the compounds indicated for 10 min at 37 °C and PMCA-, SERCA-, SPCA-, or GlyT2-specific activities were measured as detailed under "Experimental Procedures." ALX1393 concentrations in *A* and *B* were 1 μM; KB-mes concentration in *B* was 10 μM, and caloxin 2a1 concentration in *C* was 400 μM. GlyT2 transport in *A* is shown as total [^{3}H]glycine counts in a 10-min assay in the presence of *N*[3-(4′-fluorophenyl)-3-(4′-phenylphenoxy)propyl]sarcosine (GlyT1 inhibitor). *Bars* represent S.E. of triplicates from at least three different experiments. **, significantly different from control, $p < 0.01$; ***, significantly different from control, $p < 0.001$; *n.s.*, not significantly different from control by ANOVA using Tukey's post hoc test. *Veh,* vehicle.

PMCA/NCX1-mediated regulation of GlyT2 was dependent on lipid raft integrity. A common approach used to disrupt raft structures is based on the use of methyl-β-cyclodextrin (MβCD), a cholesterol chelator that extracts cholesterol from the plasma membrane disassembling raft structures (58, 78–80). Brainstem and spinal cord synaptosomes were incubated with different concentrations of MβCD (0–2 and 5 mM) with or without caloxin 2a1 (Fig. 9, *A* and *B*) or KB-mes (Fig. 9,

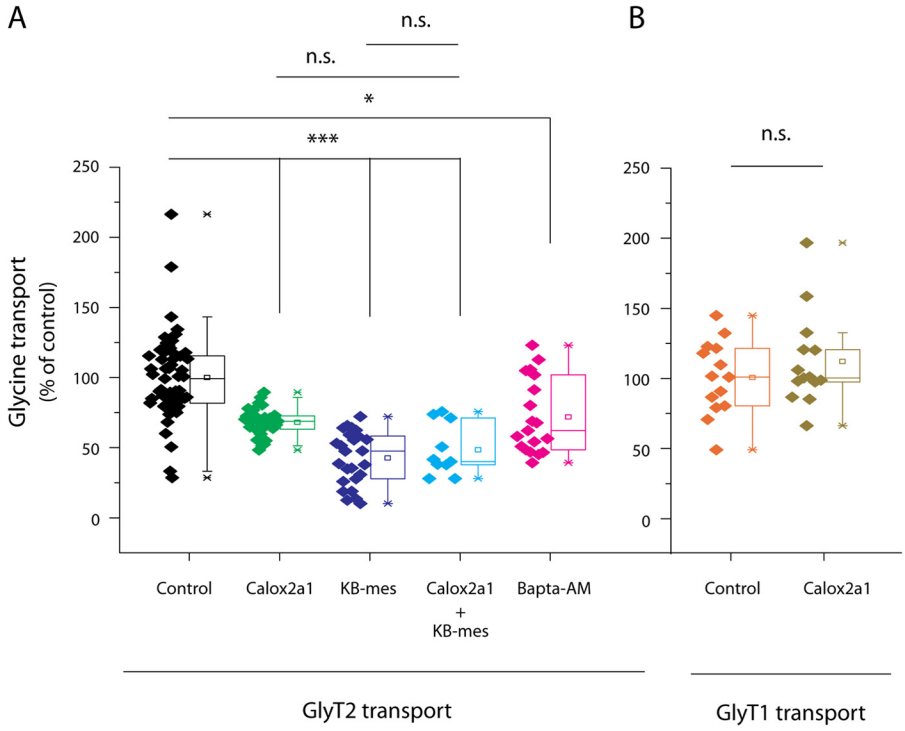

FIGURE 7. **PMCA and NCX activities modulate GlyT2 transport of glycine.** *A,* synaptosomes from the rat brainstem and spinal cord were incubated with vehicle (*control, n* = 60, *black*) or 400 μM caloxin 2a1 (*calox2a1*, *n* = 31, *green*), 10 μM KB-mes (*n* = 25, *purple*), both compounds at those concentrations (*n* = 11, *blue*) or 20 μM BAPTA-AM (*n* = 19, *pink*). The glycine uptake by GlyT2 was then measured. 100% glycine transport by GlyT2 was 51.30 ± 1.97 pmol of Gly/mg of protein/min. *B,* synaptosomes from the rat cortex were incubated in presence of vehicle (*control*, *n* = 14, *orange*) or 400 μM caloxin 2a1 (*calox2a1*, *n* = 14, *brown*). The glycine uptake by GlyT1 was then measured. 100% of activity was 4.07 ± 0.24 pmol of Gly/mg of protein/min. *, significantly different from control, $p < 0.05$; ***, significantly different from control, $p < 0.001$; *n.s.*, not significantly different. Comparisons of the means were performed using ANOVA by Tukey's post hoc test.

C and *D*). Inhibition of GlyT2 activity by caloxin 2a1 or KB-mes was blocked in a dose-dependent manner (Fig. 9, *A* and *C*), showing a complete blockage of the inhibition with 5 mM MβCD treatments (Fig. 9*B*, caloxin2a1 + MβCD remaining transport 97.74 ± 14.39% S.E., $p = 0.9998$; Fig. 9*D*, KB-mes + MβCD remaining transport 91.15 ± 17.45% S.E., $p = 0.9986$), which points out the importance of raft structures for the GlyT2/NCX/PMCA interplay. To further support these results, we studied the effect of MβCD on the co-localization of GlyT2/PMCA/NCX in primary neurons. The treatment used in this work (5 mM, 30 min) has been previously shown to reorganize GlyT2 in primary neurons, showing a specific punctae redistribution that is not observed in other neuronal markers such as MAP2 and that is independent of cellular toxicity (11). We measured Pearson's values on MβCD-treated and -untreated cells and observed a significant reduction in the co-localization of GlyT2 with PMCA2 (*B*, $p = 0.00167$), PMCA3 (*D*, $p = 0.00109$), and NCX (*F*, $p = 6.33 \times 10^{-5}$), suggesting a reduction in the local compartmentalization of these proteins (Fig. 10, *A–F*).

Together, these results show that caloxin2a1 and KB-mes-mediated inhibitions of GlyT2 need lipid raft integrity, and they suggest that spatial compartmentalization of these proteins favors the functional coupling between them.

DISCUSSION

In this study, we have used high throughput mass spectrometry to identify proteins that interact with GlyT2 in CNS preparations to unravel new mechanisms that might modulate GlyT2 function. In this way, we have identified PMCA isoforms 2 and 3 as new protein partners of GlyT2. Reciprocal co-immunoprecipitation, immunohistochemical studies, and immunocytochemical experiments further confirmed proteomic data and indicated that GlyT2 associates and co-localizes with PMCA2 and PMCA3, whereas the interaction with the ubiquitously expressed PMCA4 isoform could not be found. Both PMCAs 2 and 3 are mainly expressed in the CNS and localize pre- and post-synaptically where they are proposed to function as calcium controllers for Ca^{2+}-driven vesicle exocytosis and neuronal Ca^{2+}-dependent regulatory mechanisms (52–54, 81). Besides this important role, PMCA2 also appears to be crucial for the survival of spinal cord cells, in particular motor neurons, under pathological conditions (82). In addition, PMCA2 genetic alterations have been described as a cause of human deafness (83, 84), and recently, a genetic alteration of isoform 3 of PMCAs was identified in a family with X-linked congenital cerebellar ataxia (54).

One important finding of this work is that GlyT2 not only interacts with PMCA2/3 isoforms but also with NCX1, an exchanger ubiquitously distributed through the CNS with a crucial role for intracellular calcium homeostasis (66, 85). These protein interactions are probably enriched in lipid raft membrane subdomains, as suggested both by triple co-localization between GlyT2, PMCA2/PMCA3/NCX1, and the neuronal raft marker Thy-1 and through the dependence on lipid raft

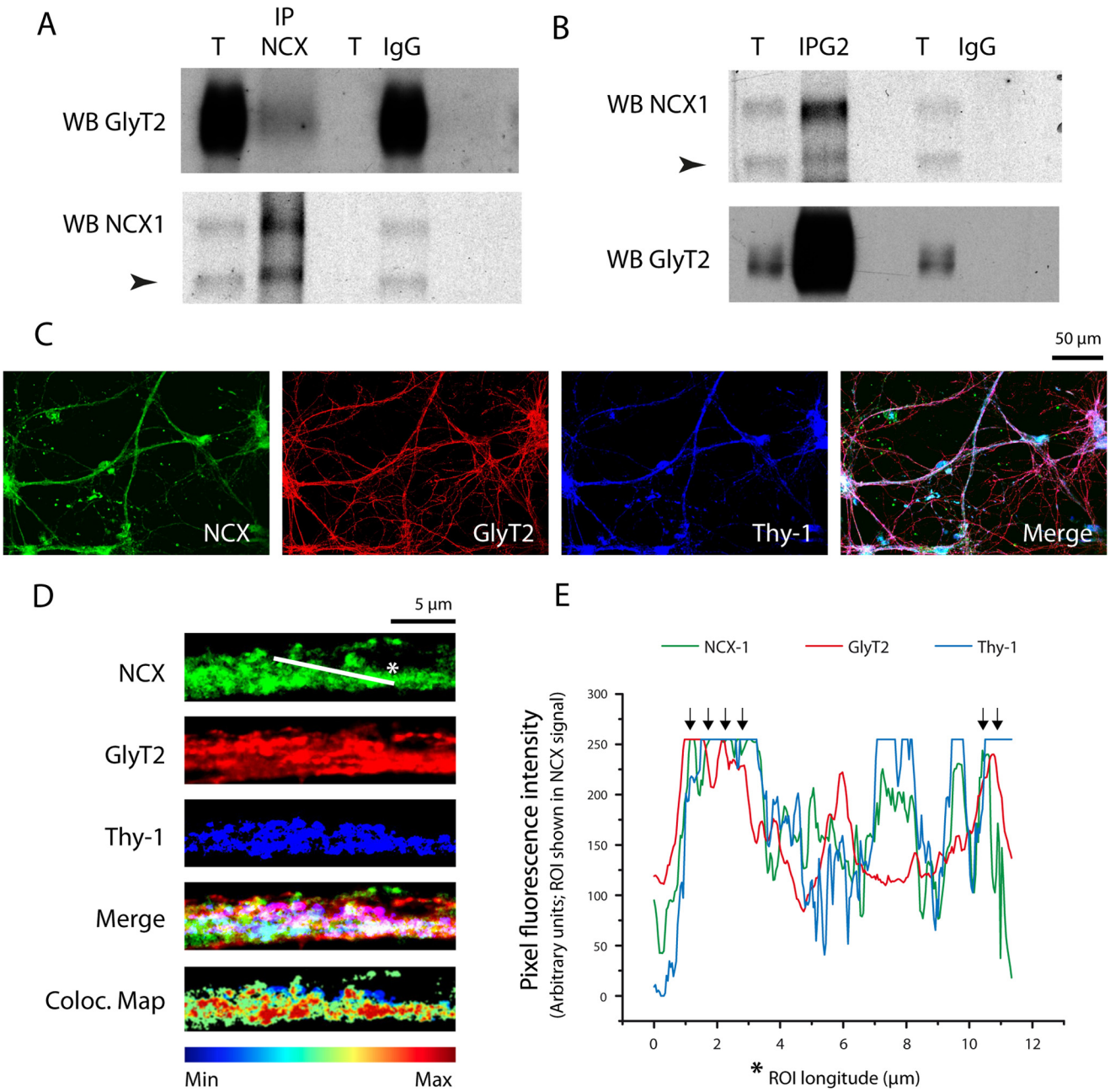

FIGURE 8. **GlyT2 interacts with the Na^+/Ca^{2+} exchanger (NCX) and both proteins are present in the same neuronal membrane raft clusters.** *A* and *B*, synaptosomes from the rat brainstem and spinal cord were lysed and incubated with antibodies against NCX1 (*A*) or GlyT2 (*B*) or the equivalent IgGs as control (*A* and *B*). Precipitated protein complexes were analyzed in Western blots (*WB*) probed with anti-GlyT2 or anti-NCX1 antibodies. *T*, total protein; *IP*, immunoprecipitated sample; *IgG*, IgG immunoprecipitation controls. Note that two bands are observed in NCX1 Western blots that correspond to the full-length protein (highlighted by an *arrowhead*, 100 kDa) and the nonreduced protein around 160 kDa (96). *C–E*, primary cultures of spinal cord and brainstem neurons were fixed and incubated with primary and secondary antibodies against NCX1 (*green*), GlyT2 (*red*), and the lipid raft marker Thy-1 (*blue*). Cells were visualized by confocal microscopy, and amplified high definition images of axonal regions were taken to generate triple co-localization maps. Top panel indicated ROI longitude that is represented in the *abscissa* of *E*. *E*, pixel fluorescence intensity profiles were generated to visualize co-distribution of GlyT2 and NCX1 in Thy-1-positive clusters. The linear region of interest (*ROI*) was manually drawn from right to left, and fluorescence intensity profiles were obtained from each individual color channel. Triple co-localization spots are highlighted by *inverted arrows*. *Scale bar, C*, 50 µm. *Scale bar, D*, 5 µm.

integrity for GlyT2 inhibition during PMCA or NCX1 blockage. This membrane compartmentalization would favor the interaction between active populations of GlyT2, PMCA2/3, and NCX1, facilitating local presynaptic sodium/calcium homeostasis during glycine recapture while functioning in an ionic microdomain in which Na^+ and Ca^{2+} concentrations differ from those in the bulk cytosol (86, 87). At synapses, NCX and PMCA are the two only plasma membrane proteins responsible for Ca^{2+} extrusion and work together to control the recovery of Ca^{2+} basal levels in the small compartment of axon terminals. They have complementary functional characteristics, whereas the PMCA has high Ca^{2+} affinity and low transport capacity, NCX has low Ca^{2+} affinity but high capacity for Ca^{2+} transport (88). NCX is highly expressed in presynaptic terminals where it is very active (89). Under basal conditions, NCX transports $3Na^+$ into the cell and extrudes $1Ca^{2+}$ from the cytoplasm

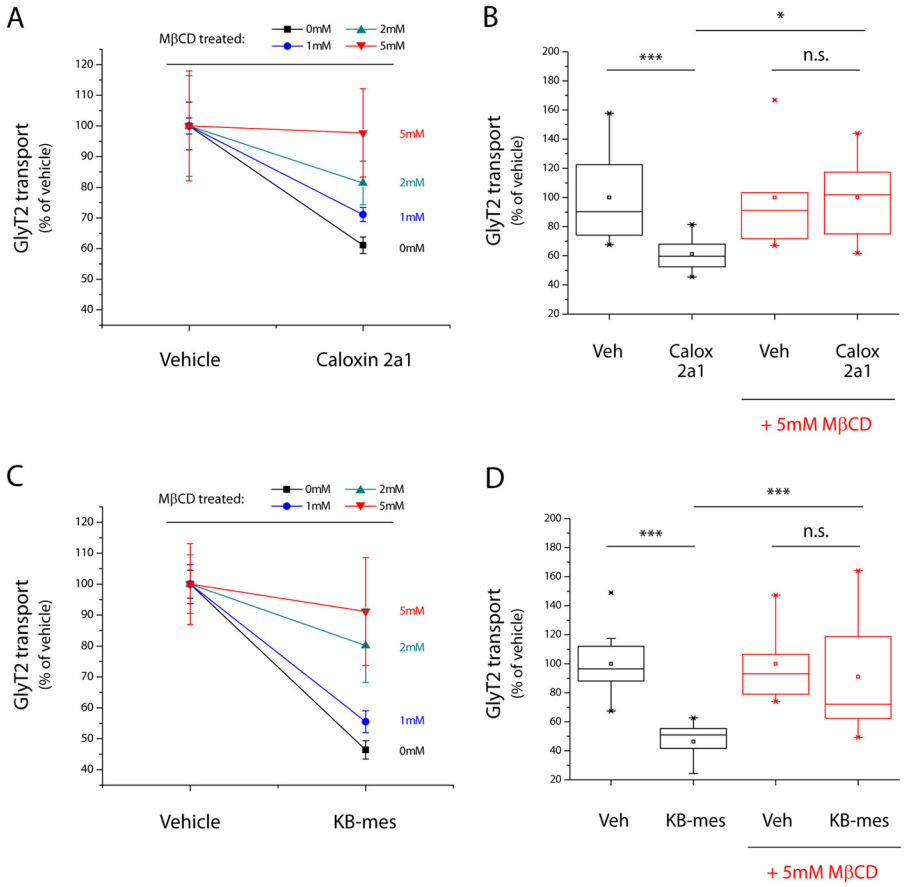

FIGURE 9. **PMCA and NCX regulation of GlyT2 activity depends on lipid raft integrity.** *A–D* synaptosomes from the rat brainstem and spinal cord were incubated in the presence of vehicle (*Veh*), caloxin 2a1 (*Calox 2A1*) (*A* and *B*), or KB-mes (*C* and *D*) with or without increasing concentrations of MβCD (1, 2, and 5 mM). The glycine uptake by GlyT2 was then measured. Each vehicle condition (0, 1, 2, and 5 mM MβCD) was normalized to 100%, having vehicle GlyT2 activities of 51.30 ± 1.97, 45.32 ± 1.19, 21.47 ± 3.53, and 5.30 ± 0.95 pmol of Gly/mg of protein/min, respectively, accordingly to published results (11). *Bars* represent S.E. of triplicates from at least three different experiments in *A* and *C*. *B,* box whisker plot showing differences in GlyT2 transport in vehicle (*veh*) and caloxin 2a1 compared with vehicle and caloxin 2a1 in the presence of 5 mM MβCD. Note that inhibition produced by caloxin 2a1 (*black*) is reversed in the presence of 5 mM MβCD, reaching a 97.74% ± 14.40 of vehicle activity. *D,* box whisker plot showing differences in GlyT2 transport in vehicle (*veh*) and KB-mes compared with vehicle and KB-mes in the presence of 5 mM MβCD. Note that inhibition produced by KB-mes (*black*) is reversed in the presence of 5 mM MβCD, reaching a 91.15 ± 17.45% of vehicle activity. *, significantly different from control, $p < 0.05$; ***, significantly different from control, $p < 0.001$; *n.s.*, not significantly different. Comparisons of the means were performed using ANOVA by Tukey's post hoc test.

functioning in the "forward mode." However, under certain physiological conditions such as neuronal activity, intracellular Na^+ increases can switch NCX to function in the "reverse mode" to expel Na^+ excess (Ca^{2+} influx, Na^+ efflux) (71, 72). Thus, it is conceivable that local increases in intracellular Na^+ in similar conditions could switch NCX from its forward mode to its reverse mode of action.

The results presented in this paper lead us to propose the existence of a functional complex where GlyT2 would be tightly coupled to PMCA and NCX to promote Na^+ and Ca^{2+} homeostasis in specific microdomains of the presynaptic glycinergic membranes (Fig. 11*A*). In this regard, the decrease in GlyT2 transport activity caused by caloxin 2a1 and KB-mes (selective inhibitors of PMCA and reversed NCX, respectively) suggests that when PMCA and NCX are inhibited, GlyT2 activity could be directly affected by local changes in Na^+/Ca^{2+} gradients due to a decrease in the Na^+ driving force necessary for glycine transport and/or be inactivated by an unknown Na^+- and/or Ca^{2+}-mediated signaling mechanism that would block glycine recapture. Independently of the molecular mechanism, similar homeostatic regulation has been proposed for other proteins, as the interplay between AMPA receptors and the Na^+/Ca^{2+} exchanger in neocortical interneurons (90), and the interaction between PMCA2 and nicotinic acetylcholine receptors in hippocampal interneurons (91).

It has been previously shown that PMCA isoforms participate in multiprotein complexes at the cell membrane (27). PMCA2 interacts presynaptically with syntaxin-1A, a member of the SNARE complex, and postsynaptically with the scaffolding protein PSD95 (52). Given its fast Ca^{2+} activation kinetics, PMCA2 is especially suited for rapid clearance of presynaptic Ca^{2+} in fast-spiking inhibitory nerve terminals (51). Therefore, its association with syntaxin-1A may provide PMCA2 a docking place close to the site of neurotransmitter release where precise and rapid control of presynaptic Ca^{2+} levels is crucial for neurotransmission (18). It should be noted that some years ago we reported an interaction between GlyT2 and syntaxin-1A that is involved in a calcium-dependent rapid increase of the amount of GlyT2 in the presynaptic membrane during neuronal activity. The GlyT2/syntaxin-1A interaction favors the rapid reuptake and recycling of glycine into the nerve terminal (16). Thus GlyT2, syntaxin-1A, and PMCA2 could be forming a

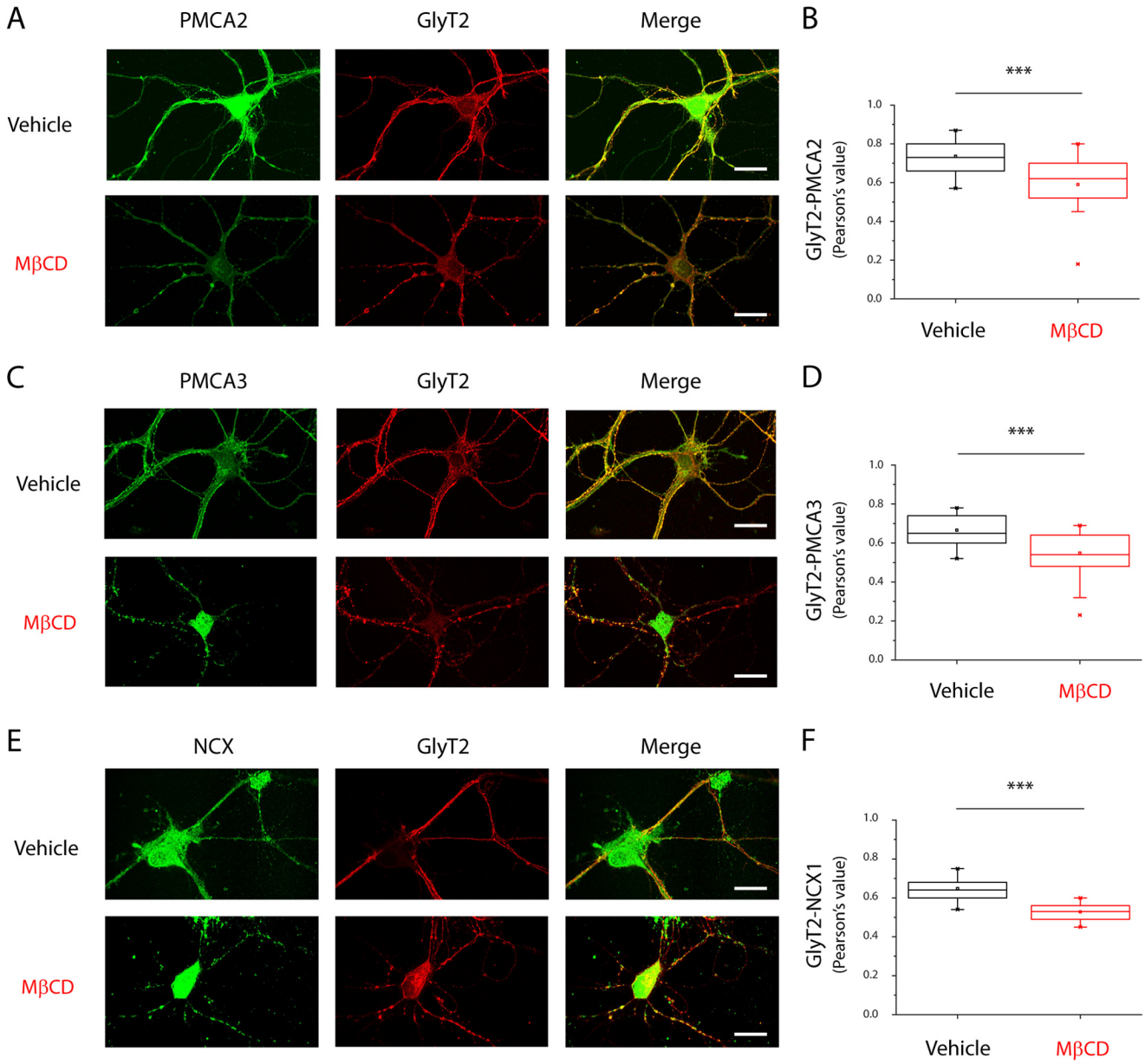

FIGURE 10. **Disruption of lipid raft integrity reduces co-localization of GlyT2 with NCX, PMCA2, and PMCA3 in primary cultures of neurons.** *A–F*, primary cultures of spinal cord and brainstem neurons were treated with 5 mM MβCD during 30 min, fixed, and incubated with primary and secondary antibodies against GlyT2 and PMCA2 (*A*), PMCA3 (*C*), or NCX (*E*). Cells were visualized by confocal microscopy, and images of primary neurons were taken. *Scale bar*, 50 μm. *B, C,* and *F,* quantification of the co-localization using Pearson's value was performed as described under "Experimental Procedures." The box whisker plots show differences on the co-localization between GlyT2 and PMCA2 (*B*), PMCA3 (*D*), and NCX (*F*). ***, significantly different from control, $p < 0.001$. Comparisons of the means were performed using ANOVA by Tukey's post hoc test ($n = 3$; on average, 20 images per condition were analyzed in each experiment).

presynaptic protein complex that would regulate GlyT2 via controlling both activity and surface expression of the transporter during neurotransmitter release.

Considering our recent identification of NKA as a partner for GlyT2 that modulates endocytosis and expression of the transporter (15), the above discussion raises the exciting possibility that GlyT2 interactions described so far with syntaxin-1A, NKA, PMCA, and NCX could occur within the same presynaptic surface complex. In agreement with this hypothesis, an interaction between NCX and NKA has also been reported (92–95). Moreover, NCX-NKA coupling has been proposed to facilitate local intracellular calcium regulation in specific and dynamic calcium signaling microdomains where lipid composition and lipid/protein interactions play an important role (87). As a compendium of these protein-protein couplings, a scheme of the physical and functional interplay between NKA, NCX, PMCA, STX1A, and GlyT2 is shown in Fig. 11*B*.

In summary, as proposed in Fig. 11*A*, binding of GlyT2 to PMCA isoforms 2 and 3 and to the NCX1 in lipid raft subdomains is postulated to help in the local homeostasis of Na^+ and Ca^{2+} during high rates of GlyT2-mediated recapture of glycine in presynaptic terminals. After neurotransmitter release, active raft-associated GlyT2 reuptakes large amounts of glycine back to the terminal producing Na^+ imbalances that must be restored. In normal conditions, this recovery is performed by Na^+/K^+-ATPase, but the pump can be saturated in

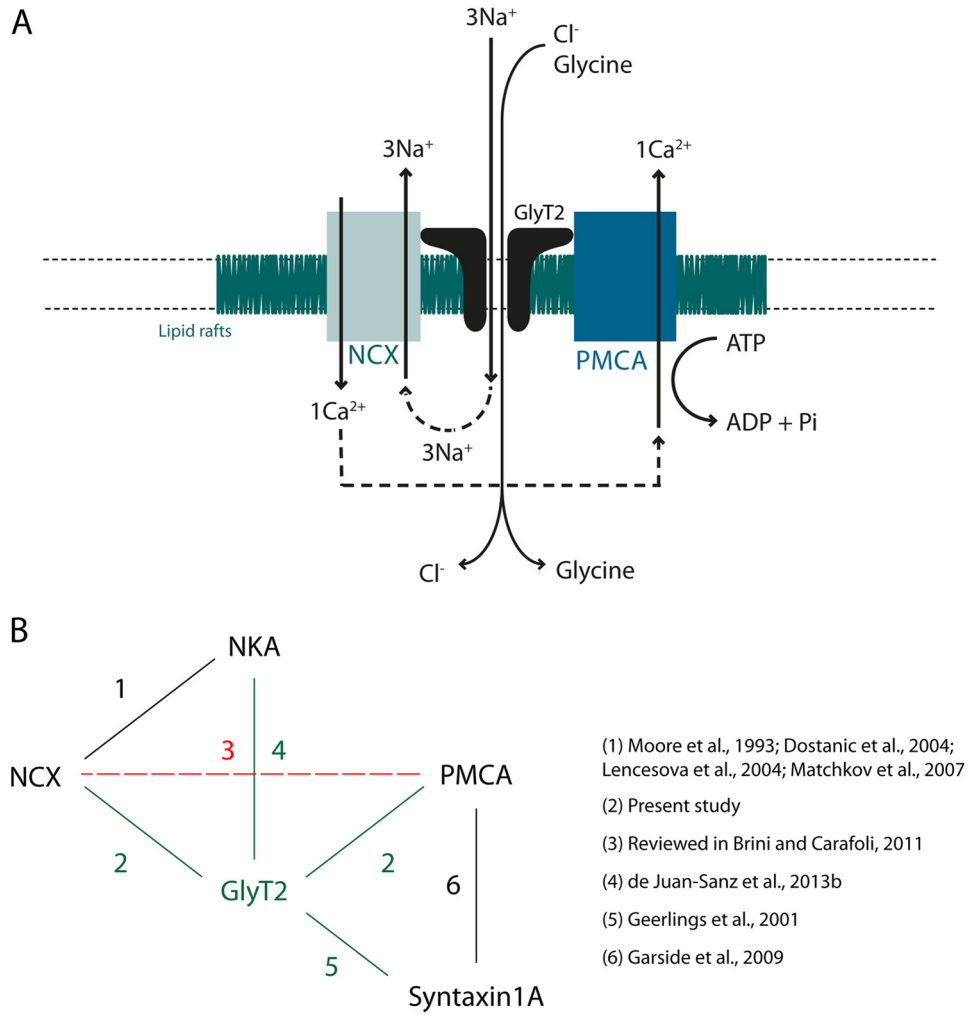

FIGURE 11. **Proposed functional relationship between GlyT2, NCX, and PMCAs in glycinergic terminals and functional interplay between NKA, NCX, PMCA, STX1A, and GlyT2.** *A,* putative model of a glycinergic terminal showing the GlyT2·NCX·PMCA complex (*black/green/blue*, respectively). *Arrows* indicate the movement of neurotransmitter and ions. The *hatched area* represent lipid rafts subdomains in the plasma membrane. *B,* scheme of physical and functional interplay between GlyT2 interacting proteins. GlyT2 interactions are denoted by *green lines* (*2, 4* and *5*). Interactions between GlyT2 interacting proteins are denoted by *black lines* (1, 6). NCX and PMCA have not been shown to physically interact, but they are highly related functionally, and this is denoted by a *dashed line* in *red* (3). Legend at *right* shows the references where these interactions are described.

situations of strong demand due to its low rates of transport (200 Hz) (37). We propose that under these conditions of saturation, Na^+ is extruded out of the terminal by NCX (a much faster Na^+-transporting protein, 2000–5000 Hz) (88). This protein would work locally in the reverse mode introducing $1Ca^{2+}$ ion while extruding $3Na^+$ ions per cycle from the terminal. The local compartmentalization of PMCAs in these membrane raft domains would facilitate the extrusion of the Ca^{2+} ion introduced by NCX, locally balancing Ca^{2+} concentration in these situations of high glycine recapture.

Acknowledgments—We thank Dr. Ana Isabel Marina and Carlos García from the Proteomic Service of Centro de Biología Molecular Severo Ochoa for their valuable and expert assistance in the proteomic analysis; Dr. Jesús Vazquez from the Centro Nacional de Investigaciones Cardiovasculares for helpful suggestions, and Dr. Michael B. Hoppa (Dartmouth University) for valuable discussions and comments on the manuscript.

REFERENCES

1. Zafra, F., Aragón, C., Olivares, L., Danbolt, N. C., Giménez, C., and Storm-Mathisen, J. (1995) Glycine transporters are differentially expressed among CNS cells. *J. Neurosci.* **15,** 3952–3969
2. Aragón, C., and López-Corcuera, B. (2005) Glycine transporters: crucial roles of pharmacological interest revealed by gene deletion. *Trends Pharmacol. Sci.* **26,** 283–286
3. Gomeza, J., Ohno, K., Hülsmann, S., Armsen, W., Eulenburg, V., Richter, D. W., Laube, B., and Betz, H. (2003) Deletion of the mouse glycine transporter 2 results in a hyperekplexia phenotype and postnatal lethality. *Neuron* **40,** 797–806
4. Rousseau, F., Aubrey, K. R., and Supplisson, S. (2008) The glycine transporter GlyT2 controls the dynamics of synaptic vesicle refilling in inhibitory spinal cord neurons. *J. Neurosci.* **28,** 9755–9768
5. Apostolides, P. F., and Trussell, L. O. (2013) Rapid, activity-independent turnover of vesicular transmitter content at a mixed glycine/GABA synapse. *J. Neurosci.* **33,** 4768–4781
6. Rees, M. I., Harvey, K., Pearce, B. R., Chung, S.-K., Duguid, I. C., Thomas, P., Beatty, S., Graham, G. E., Armstrong, L., Shiang, R., Abbott, K. J., Zuberi, S. M., Stephenson, J. B., Owen, M. J., Tijssen, M. A., van den Maagdenberg, A. M., Smart, T. G., Supplisson, S., and Harvey, R. J. (2006) Mutations in the gene encoding GlyT2 (SLC6A5) define a presynaptic

component of human startle disease. *Nat. Genet.* **38,** 801–806
7. Carta, E., Chung, S.-K., James, V. M., Robinson, A., Gill, J. L., Remy, N., Vanbellinghen, J.-F., Drew, C. J., Cagdas, S., Cameron, D., Cowan, F. M., Del Toro, M., Graham, G. E., Manzur, A. Y., Masri, A., Rivera, S., Scalais, E., Shiang, R., Sinclair, K., Stuart, C. A., Tijssen, M. A., Wise, G., Zuberi, S. M., Harvey, K., Pearce, B. R., Topf, M., Thomas, R. H., Supplisson, S., Rees, M. I., and Harvey, R. J. (2012) Mutations in the GlyT2 gene (SLC6A5) are a second major cause of startle disease. *J. Biol. Chem.* **287,** 28975–28985
8. Giménez, C., Pérez-Siles, G., Martínez-Villarreal, J., Arribas-González, E., Jiménez, E., Núñez, E., de Juan-Sanz, J., Fernández-Sánchez, E., García-Tardón, N., Ibáñez, I., Romanelli, V., Nevado, J., James, V. M., Topf, M., Chung, S.-K., Thomas, R. H., Desviat, L. R., Aragón, C., Zafra, F., Rees, M. I., Lapunzina, P., Harvey, R. J., and López-Corcuera, B. (2012) A novel dominant hyperekplexia mutation Y705C alters trafficking and biochemical properties of the presynaptic glycine transporter GlyT2. *J. Biol. Chem.* **287,** 28986–29002
9. Fornés, A., Núñez, E., Alonso-Torres, P., Aragón, C., and López-Corcuera, B. (2008) Trafficking properties and activity regulation of the neuronal glycine transporter GLYT2 by protein kinase C. *Biochem. J.* **412,** 495–506
10. de Juan-Sanz, J., Zafra, F., López-Corcuera, B., and Aragón, C. (2011) Endocytosis of the neuronal glycine transporter GLYT2: role of membrane rafts and protein kinase C-dependent ubiquitination. *Traffic* **12,** 1850–1867
11. Núñez, E., Alonso-Torres, P., Fornés, A., Aragón, C., and López-Corcuera, B. (2008) The neuronal glycine transporter GLYT2 associates with membrane rafts: functional modulation by lipid environment. *J. Neurochem.* **105,** 2080–2090
12. Jiménez, E., Zafra, F., Pérez-Sen, R., Delicado, E. G., Miras-Portugal, M. T., Aragón, C., and López-Corcuera, B. (2011) P2Y purinergic regulation of the glycine neurotransmitter transporters. *J. Biol. Chem.* **286,** 10712–10724
13. de Juan-Sanz, J., Núñez, E., López-Corcuera, B., and Aragón, C. (2013) Constitutive endocytosis and turnover of the neuronal glycine transporter GlyT2 is dependent on ubiquitination of a C-terminal lysine cluster. *PLoS One* **8,** e58863
14. Arribas-González, E., Alonso-Torres, P., Aragón, C., and López-Corcuera, B. (2013) Calnexin-assisted biogenesis of the neuronal glycine transporter 2 (GlyT2). *PLoS One* **8,** e63230
15. de Juan-Sanz, J., Núñez, E., Villarejo-López, L., Pérez-Hernández, D., Rodriguez-Fraticelli, A. E., López-Corcuera, B., Vázquez, J., and Aragón, C. (2013) Na^+/K^+-ATPase is a new interacting partner for the neuronal glycine transporter GlyT2 that downregulates its expression *in vitro* and *in vivo*. *J. Neurosci.* **33,** 14269–14281
16. Geerlings, A., Núñez, E., López-Corcuera, B., and Aragón, C. (2001) Calcium- and syntaxin 1-mediated trafficking of the neuronal glycine transporter GLYT2. *J. Biol. Chem.* **276,** 17584–17590
17. Dittman, J., and Ryan, T. A. (2009) Molecular circuitry of endocytosis at nerve terminals. *Annu. Rev. Cell Dev. Biol.* **25,** 133–160
18. Ariel, P., and Ryan, T. A. (2012) New insights into molecular players involved in neurotransmitter release. *Physiology* **27,** 15–24
19. Berridge, M. J., Lipp, P., and Bootman, M. D. (2000) The versatility and universality of calcium signalling. *Nat. Rev. Mol. Cell Biol.* **1,** 11–21
20. Augustine, G. J., Santamaria, F., and Tanaka, K. (2003) Local calcium signaling in neurons. *Neuron* **40,** 331–346
21. Bading, H. (2013) Nuclear calcium signalling in the regulation of brain function. *Nat. Rev. Neurosci.* **14,** 593–608
22. Mata, A. M., Berrocal, M., and Sepúlveda, M. R. (2011) Impairment of the activity of the plasma membrane Ca^{2+}-ATPase in Alzheimer's disease. *Biochem. Soc. Trans.* **39,** 819–822
23. Berrocal, M., Sepulveda, M. R., Vazquez-Hernandez, M., and Mata, A. M. (2012) Calmodulin antagonizes amyloid-β peptides-mediated inhibition of brain plasma membrane Ca^{2+}-ATPase. *Biochim. Biophys. Acta* **1822,** 961–969
24. Tidow, H., Poulsen, L. R., Andreeva, A., Knudsen, M., Hein, K. L., Wiuf, C., Palmgren, M. G., and Nissen, P. (2012) A bimodular mechanism of calcium control in eukaryotes. *Nature* **491,** 468–472
25. Bublitz, M., Musgaard, M., Poulsen, H., Thøgersen, L., Olesen, C., Schiøtt, B., Morth, J. P., Møller, J. V., and Nissen, P. (2013) Ion pathways in the sarcoplasmic reticulum Ca^{2+}-ATPase. *J. Biol. Chem.* **288,** 10759–10765
26. Vandecaetsbeek, I., Vangheluwe, P., Raeymaekers, L., Wuytack, F., and Vanoevelen, J. (2011) The Ca^{2+} pumps of the endoplasmic reticulum and Golgi apparatus. *Cold Spring Harb. Perspect. Biol.* **3,** a004184
27. Strehler, E. E., Caride, A. J., Filoteo, A. G., Xiong, Y., Penniston, J. T., and Enyedi, A. (2007) Plasma membrane Ca^{2+}-ATPases as dynamic regulators of cellular calcium handling. *Ann. N.Y. Acad. Sci.* **1099,** 226–236
28. Strehler, E. E., Filoteo, A. G., Penniston, J. T., and Caride, A. J. (2007) Plasma-membrane Ca^{2+} pumps: structural diversity as the basis for functional versatility. *Biochem. Soc. Trans.* **35,** 919–922
29. Strehler, E. E., and Zacharias, D. A. (2001) Role of alternative splicing in generating isoform diversity among plasma membrane calcium pumps. *Physiol. Rev.* **81,** 21–50
30. Mata, A. M., and Sepúlveda, M. R. (2005) Calcium pumps in the central nervous system. *Brain Res. Brain Res. Rev.* **49,** 398–405
31. Sepúlveda, M. R., Berrocal-Carrillo, M., Gasset, M., and Mata, A. M. (2006) The plasma membrane Ca^{2+}-ATPase isoform 4 is localized in lipid rafts of cerebellum synaptic plasma membranes. *J. Biol. Chem.* **281,** 447–453
32. Jiang, L., Fernandes, D., Mehta, N., Bean, J. L., Michaelis, M. L., and Zaidi, A. (2007) Partitioning of the plasma membrane Ca^{2+}-ATPase into lipid rafts in primary neurons: effects of cholesterol depletion. *J. Neurochem.* **102,** 378–388
33. Jiang, L., Bechtel, M. D., Galeva, N. A., Williams, T. D., Michaelis, E. K., and Michaelis, M. L. (2012) Decreases in plasma membrane Ca^{2+}-ATPase in brain synaptic membrane rafts from aged rats. *J. Neurochem.* **123,** 689–699
34. Tortelote, G. G., Valverde, R. H., Lemos, T., Guilherme, A., Einicker-Lamas, M., and Vieyra, A. (2004) The plasma membrane Ca^{2+} pump from proximal kidney tubules is exclusively localized and active in caveolae. *FEBS Lett.* **576,** 31–35
35. Zhang, J., Xiao, P., and Zhang, X. (2009) Phosphatidylserine externalization in caveolae inhibits Ca^{2+} efflux through plasma membrane Ca^{2+}-ATPase in ECV304. *Cell Calcium* **45,** 177–184
36. Fujimoto, T. (1993) Calcium pump of the plasma membrane is localized in caveolae. *J. Cell Biol.* **120,** 1147–1157
37. Skou, J. C. (1990) The energy coupled exchange of Na^+ for K^+ across the cell membrane. *FEBS Lett.* **268,** 314–324
38. Hilgemann, D. W., Nicoll, D. A., and Philipson, K. D. (1991) Charge movement during Na^+ translocation by native and cloned cardiac Na^+/Ca^{2+} exchanger. *Nature* **352,** 715–718
39. Hilgemann, D. W. (1996) Unitary cardiac Na^+, Ca^{2+} exchange current magnitudes determined from channel-like noise and charge movements of ion transport. *Biophys. J.* **71,** 759–768
40. Núñez, E., Pérez-Siles, G., Rodenstein, L., Alonso-Torres, P., Zafra, F., Jiménez, E., Aragón, C., and López-Corcuera, B. (2009) Subcellular localization of the neuronal glycine transporter GLYT2 in brainstem. *Traffic* **10,** 829–843
41. Chaudhary, J., Walia, M., Matharu, J., Escher, E., and Grover, A. K. (2001) Caloxin: a novel plasma membrane Ca^{2+} pump inhibitor. *Am. J. Physiol. Cell Physiol.* **280,** C1027–C1030
42. Cubelos, B., Leite, C., Giménez, C., and Zafra, F. (2014) Localization of the glycine transporter GLYT1 in glutamatergic synaptic vesicles. *Neurochem. Int.* **73,** 204–210
43. Sepúlveda, M. R., Berrocal, M., Marcos, D., Wuytack, F., and Mata, A. M. (2007) Functional and immunocytochemical evidence for the expression and localization of the secretory pathway Ca^{2+}-ATPase isoform 1 (SPCA1) in cerebellum relative to other Ca^{2+} pumps. *J. Neurochem.* **103,** 1009–1018
44. Bolte, S., and Cordelières, F. P. (2006) A guided tour into subcellular colocalization analysis in light microscopy. *J. Microsc.* **224,** 213–232
45. Zinchuk, V., and Grossenbacher-Zinchuk, O. (2011) Quantitative colocalization analysis of confocal fluorescence microscopy images. *Curr. Protoc. Cell Biol.* 2011 Chapter 4, Unit 4.19
46. Jaskolski, F., Mulle, C., and Manzoni, O. J. (2005) An automated method to quantify and visualize colocalized fluorescent signals. *J. Neurosci. Methods* **146,** 42–49

47. Shevchenko, A., Wilm, M., Vorm, O., and Mann, M. (1996) Mass spectrometric sequencing of proteins from silver-stained polyacrylamide gels. *Anal. Chem.* **68,** 850–858
48. Bonzon-Kulichenko, E., Pérez-Hernández, D., Núñez, E., Martínez-Acedo, P., Navarro, P., Trevisan-Herraz, M., Ramos, M. del C., Sierra, S., Martínez-Martínez, S., Ruiz-Meana, M., Miró-Casas, E., García-Dorado, D., Redondo, J. M., Burgos, J. S., and Vázquez, J. (2011) A robust method for quantitative high-throughput analysis of proteomes by ^{18}O labeling. *Mol. Cell. Proteomics* **10,** M110.003335
49. Burette, A., and Weinberg, R. J. (2007) Perisynaptic organization of plasma membrane calcium pumps in cerebellar cortex. *J. Comp. Neurol.* **500,** 1127–1135
50. Jensen, T. P., Filoteo, A. G., Knopfel, T., and Empson, R. M. (2007) Presynaptic plasma membrane Ca^{2+} ATPase isoform 2a regulates excitatory synaptic transmission in rat hippocampal CA3. *J. Physiol.* **579,** 85–99
51. Burette, A. C., Strehler, E. E., and Weinberg, R. J. (2009) "Fast" plasma membrane calcium pump PMCA2a concentrates in GABAergic terminals in the adult rat brain. *J. Comp. Neurol.* **512,** 500–513
52. Garside, M. L., Turner, P. R., Austen, B., Strehler, E. E., Beesley, P. W., and Empson, R. M. (2009) Molecular interactions of the plasma membrane calcium ATPase 2 at pre- and post-synaptic sites in rat cerebellum. *Neuroscience* **162,** 383–395
53. Boczek, T., Lisek, M., Kowalski, A., Pikula, S., Niewiarowska, J., Wiktorska, M., and Zylinska, L. (2012) Downregulation of PMCA2 or PMCA3 reorganizes Ca^{2+} handling systems in differentiating PC12 cells. *Cell Calcium* **52,** 433–444
54. Zanni, G., Calì, T., Kalscheuer, V. M., Ottolini, D., Barresi, S., Lebrun, N., Montecchi-Palazzi, L., Hu, H., Chelly, J., Bertini, E., Brini, M., and Carafoli, E. (2012) Mutation of plasma membrane Ca^{2+} ATPase isoform 3 in a family with X-linked congenital cerebellar ataxia impairs Ca^{2+} homeostasis. *Proc. Natl. Acad. Sci. U.S.A.* **109,** 14514–14519
55. DeMarco, S. J., and Strehler, E. E. (2001) Plasma membrane Ca^{2+}-ATPase isoforms 2b and 4b interact promiscuously and selectively with members of the membrane-associated guanylate kinase family of PDZ (PSD95/Dlg/ZO-1) domain-containing proteins. *J. Biol. Chem.* **276,** 21594–21600
56. Di Leva, F., Domi, T., Fedrizzi, L., Lim, D., and Carafoli, E. (2008) The plasma membrane Ca^{2+} ATPase of animal cells: structure, function and regulation. *Arch. Biochem. Biophys.* **476,** 65–74
57. Enyedi, A., and Strehler, E. E. (2011) Regulation of apical membrane enrichment and retention of plasma membrane Ca ATPase splice variants by the PDZ-domain protein NHERF2. *Commun. Integr. Biol.* **4,** 340–343
58. Allen, J. A., Halverson-Tamboli, R. A., and Rasenick, M. M. (2007) Lipid raft microdomains and neurotransmitter signalling. *Nat. Rev. Neurosci.* **8,** 128–140
59. Pike, L. J. (2009) The challenge of lipid rafts. *J. Lipid Res.* **50,** S323–S328
60. Simons, K., and Sampaio, J. L. (2011) Membrane organization and lipid rafts. *Cold Spring Harb. Perspect. Biol.* **3,** a004697
61. Madore, N., Smith, K. L., Graham, C. H., Jen, A., Brady, K., Hall, S., and Morris, R. (1999) Functionally different GPI proteins are organized in different domains on the neuronal surface. *EMBO J.* **18,** 6917–6926
62. Shi, F., and Sottile, J. (2008) Caveolin-1-dependent beta1 integrin endocytosis is a critical regulator of fibronectin turnover. *J. Cell Sci.* **121,** 2360–2371
63. Dohi, T., Morita, K., Kitayama, T., Motoyama, N., and Morioka, N. (2009) Glycine transporter inhibitors as a novel drug discovery strategy for neuropathic pain. *Pharmacol. Ther.* **123,** 54–79
64. Szewczyk, M. M., Pande, J., and Grover, A. K. (2008) Caloxins: a novel class of selective plasma membrane Ca^{2+} pump inhibitors obtained using biotechnology. *Pflugers Arch.* **456,** 255–266
65. Pande, J., Szewczyk, M. M., and Grover, A. K. (2011) Allosteric inhibitors of plasma membrane Ca^{2+} pumps: Invention and applications of caloxins. *World J. Biol. Chem.* **2,** 39–47
66. Brini, M., and Carafoli, E. (2011) The plasma membrane Ca^{2+} ATPase and the plasma membrane sodium calcium exchanger cooperate in the regulation of cell calcium. *Cold Spring Harb. Perspect. Biol.* **3,** a004168
67. Liao, J., Li, H., Zeng, W., Sauer, D. B., Belmares, R., and Jiang, Y. (2012) Structural insight into the ion-exchange mechanism of the sodium/calcium exchanger. *Science* **335,** 686–690
68. Blaustein, M. P., and Lederer, W. J. (1999) Sodium/calcium exchange: its physiological implications. *Physiol. Rev.* **79,** 763–854
69. Duman, J. G., Chen, L., and Hille, B. (2008) Calcium transport mechanisms of PC12 cells. *J. Gen. Physiol.* **131,** 307–323
70. Zhong, N., Beaumont, V., and Zucker, R. S. (2001) Roles for mitochondrial and reverse mode Na^+/ Ca^{2+} exchange and the plasmalemma Ca^{2+} ATPase in post-tetanic potentiation at crayfish neuromuscular junctions. *J. Neurosci.* **21,** 9598–9607
71. Roome, C. J., Power, E. M., and Empson, R. M. (2013) Transient reversal of the sodium/calcium exchanger boosts presynaptic calcium and synaptic transmission at a cerebellar synapse. *J. Neurophysiol.* **109,** 1669–1680
72. Roome, C. J., and Empson, R. M. (2013) The contribution of the sodium-calcium exchanger (NCX) and plasma membrane Ca^{2+} ATPase (PMCA) to cerebellar synapse function. *Adv. Exp. Med. Biol.* **961,** 251–263
73. Roux, M. J., and Supplisson, S. (2000) Neuronal and glial glycine transporters have different stoichiometries. *Neuron* **25,** 373–383
74. Watano, T., Kimura, J., Morita, T., and Nakanishi, H. (1996) A novel antagonist, No. 7943, of the Na^+/Ca^{2+} exchange current in guinea-pig cardiac ventricular cells. *Br. J. Pharmacol.* **119,** 555–563
75. Iwamoto, T., Watano, T., and Shigekawa, M. (1996) A novel isothiourea derivative selectively inhibits the reverse mode of Na^+/Ca^{2+} exchange in cells expressing NCX1. *J. Biol. Chem.* **271,** 22391–22397
76. Elias, C. L., Lukas, A., Shurraw, S., Scott, J., Omelchenko, A., Gross, G. J., Hnatowich, M., and Hryshko, L. V. (2001) Inhibition of Na^+/Ca^{2+} exchange by KB-R7943: transport mode selectivity and antiarrhythmic consequences. *Am. J. Physiol. Heart Circ. Physiol.* **281,** H1334–H1345
77. Iwamoto, T., Watanabe, Y., Kita, S., and Blaustein, M. P. (2007) Na^+/Ca^{2+} exchange inhibitors: a new class of calcium regulators. *Cardiovasc. Hematol. Disord. Drug Targets* **7,** 188–198
78. Eckert, G. P. (2010) Manipulation of lipid rafts in neuronal cells. *Open Biol. J.* **3,** 32–38
79. Nothdurfter, C., Tanasic, S., Di Benedetto, B., Rammes, G., Wagner, E.-M., Kirmeier, T., Ganal, V., Kessler, J. S., Rein, T., Holsboer, F., and Rupprecht, R. (2010) Impact of lipid raft integrity on 5-HT3 receptor function and its modulation by antidepressants. *Neuropsychopharmacology* **35,** 1510–1519
80. Roh, S.-E., Hong, Y. H., Jang, D. C., Kim, J., and Kim, S. J. (2014) Lipid rafts serve as signaling platforms for mGlu1 receptor-mediated calcium signaling in association with caveolin. *Mol. Brain* **7,** 9
81. Bublitz, M., Morth, J. P., and Nissen, P. (2011) P-type ATPases at a glance. *J. Cell Sci.* **124,** 2515–2519
82. Kurnellas, M. P., Li, H., Jain, M. R., Giraud, S. N., Nicot, A. B., Ratnayake, A., Heary, R. F., and Elkabes, S. (2010) Reduced expression of plasma membrane calcium ATPase 2 and collapsin response mediator protein 1 promotes death of spinal cord neurons. *Cell Death Differ.* **17,** 1501–1510
83. Schultz, J. M., Yang, Y., Caride, A. J., Filoteo, A. G., Penheiter, A. R., Lagziel, A., Morell, R. J., Mohiddin, S. A., Fananapazir, L., Madeo, A. C., Penniston, J. T., and Griffith, A. J. (2005) Modification of human hearing loss by plasma-membrane calcium pump PMCA2. *N. Engl. J. Med.* **352,** 1557–1564
84. Ficarella, R., Di Leva, F., Bortolozzi, M., Ortolano, S., Donaudy, F., Petrillo, M., Melchionda, S., Lelli, A., Domi, T., Fedrizzi, L., Lim, D., Shull, G. E., Gasparini, P., Brini, M., Mammano, F., and Carafoli, E. (2007) A functional study of plasma-membrane calcium-pump isoform 2 mutants causing digenic deafness. *Proc. Natl. Acad. Sci. U.S.A.* **104,** 1516–1521
85. Yu, L., and Colvin, R. A. (1997) Regional differences in expression of transcripts for Na^+/Ca^{2+} exchanger isoforms in rat brain. *Mol. Brain Res.* **50,** 285–292
86. Llinás, R., Sugimori, M., and Silver, R. B. (1992) Microdomains of high calcium concentration in a presynaptic terminal. *Science* **256,** 677–679
87. Tian, J., and Xie, Z. (2008) The Na-K-ATPase and calcium-signaling microdomains. *Physiology* **23,** 205–211
88. Blaustein, M. P., Juhaszova, M., Golovina, V. A., Church, P. J., and Stanley, E. F. (2002) Na/Ca exchanger and PMCA localization in neurons and astrocytes. *Ann. N.Y. Acad. Sci.* **976,** 356–366
89. Reuter, H., and Porzig, H. (1995) Localization and functional significance of the Na^+/Ca^{2+} exchanger in presynaptic boutons of hippocampal cells in culture. *Neuron* **15,** 1077–1084

90. Goldberg, J. H., Tamas, G., Aronov, D., and Yuste, R. (2003) Calcium microdomains in aspiny dendrites. *Neuron* **40,** 807–821
91. Gómez-Varela, D., Schmidt, M., Schoellerman, J., Peters, E. C., and Berg, D. K. (2012) PMCA2 via PSD-95 controls calcium signaling by α7-containing nicotinic acetylcholine receptors on aspiny interneurons. *J. Neurosci.* **32,** 6894–6905
92. Moore, E. D., Etter, E. F., Philipson, K. D., Carrington, W. A., Fogarty, K. E., Lifshitz, L. M., and Fay, F. S. (1993) Coupling of the Na^+/Ca^{2+} exchanger, Na^+/K^+ pump and sarcoplasmic reticulum in smooth muscle. *Nature* **365,** 657–660
93. Dostanic, I., Schultz Jel, J., Lorenz, J. N., and Lingrel, J. B. (2004) The α1 isoform of Na,K-ATPase regulates cardiac contractility and functionally interacts and co-localizes with the Na/Ca exchanger in heart. *J. Biol. Chem.* **279,** 54053–54061
94. Lencesova, L., O'Neill, A., Resneck, W. G., Bloch, R. J., and Blaustein, M. P. (2004) Plasma membrane-cytoskeleton-endoplasmic reticulum complexes in neurons and astrocytes. *J. Biol. Chem.* **279,** 2885–2893
95. Matchkov, V. V., Gustafsson, H., Rahman, A., Briggs Boedtkjer, D. M., Gorintin, S., Hansen, A. K., Bouzinova, E. V., Praetorius, H. A., Aalkjaer, C., and Nilsson, H. (2007) Interaction between Na^+/K^+-pump and Na^+/Ca^{2+}-exchanger modulates intercellular communication. *Circ. Res.* **100,** 1026–1035
96. Philipson, K. D., Longoni, S., and Ward, R. (1988) Purification of the cardiac Na^+- Ca^{2+} exchange protein. *Biochim. Biophys. Acta* **945,** 298–306